Prog. Oceanog. Vol. 31, pp. 1-50, 1993.
Printed in Great Britain. All rights reserved.

0079 - 6611/93 $24.00

A census of eddies observed in North Atlantic SOFAR float data

P.L. RICHARDSON

Woods Hole Oceanographic Institution, Woods Hole, Massachusetts 02543, USA

Abstract – SOFAR floats that looped in discrete eddies were studied in order to map and describe the distribution and characteristics of eddies in the North Atlantic. One hundred eighteen individual looping float trajectories (loopers) were identified, each consisting of two or more consecutive loops. Each looper was interpreted to be in a discrete eddy, and its characteristics were estimated from the float trajectory. The highest percentage of loopers occurred at 700m in the Newfoundland Basin, where roughly half of the float data were in loopers, mostly cyclones. In the Gulf Stream region, approximately 20% of the float data recorded at 700m were in loopers, again mostly cyclones. Overall, 21% of 700m data and 6% of 2000m data were in loopers.

The fastest swirl speeds, >40cm s^{-1}, were in cyclones south of the Gulf Stream (most of which were in Gulf Stream rings), but numerous swift ~35cm s^{-1} anticyclones were found there too. Swirl velocity decreased with depth, to roughly half as swift at 2000m as at 700m for three eddies in the Sargasso Sea measured simultaneously with floats at these two depths. In the western North Atlantic, the average swirl velocity of cyclones and anticyclones was the same.

Translation velocity of eddies was generally westward to southwestward at a few cm s^{-1}. The mean translation velocity of 39 eddies in the Sargasso Sea was $\overline{u} = -2.8 \pm 0.4$cm s^{-1}, $\overline{v} = -0.4 \pm 0.4$cm s^{-1}. Many of these were located just south of the Gulf Stream in the region of its recirculation and were probably advected by a westward current there. Near the Gulf Stream and along its extension in the Newfoundland Basin, eddies were often advected downstream with speeds up to 15-20cm s^{-1} and eddy trajectories were often complicated. South of 30°N and near the western boundary, 700m eddies were advected northwestward and 1300m and 2000m eddies southeastward by boundary currents there.

Numerous energetic anticyclones were observed south of the Gulf Stream; one was tracked for 430 days and its properties well measured. The formation of these eddies has not been documented, but they are inferred to have formed near and by the Gulf Stream and to consist of a thick layer of 18°C water lying above a depression in the thermocline. Analogous anticyclones were observed in the Newfoundland Basin seaward of the Gulf Stream extension there.

CONTENTS

1. INTRODUCTION

The great difficulty in following discrete eddies in the ocean has resulted in their life histories and trajectories remaining largely unknown. This is especially true of interior or subsurface eddies. During the last few years, numerous freely drifting neutrally buoyant SOund Fixing and Ranging (SOFAR) floats have become trapped and have looped for various lengths of time in discrete eddies, thus revealing new information about their paths and histories. A few of the trajectories have been described in the literature (OWENS, 1991; RICHARDSON, WALSH, ARMI, SCHRÖDER and PRICE, 1989) but most have not been inadequately studied, especially those seen in recent data in the vicinity of the Gulf Stream.

This present study systematically identifies U.S. SOFAR floats which have looped in what are interpreted as being discrete eddies. Several new and interesting eddy case histories are described, all the eddies are mapped and their statistical properties explored. Results reveal new information concerning the number, distribution, and trajectories of discrete eddies in the North Atlantic. Although the life histories of some eddies are complicated, when the data are pooled we begin to see distinctive patterns.

Floats are a unique tool to study eddies. When a float becomes trapped in the rotating swirl flow around an eddy's centre, the path of the eddy itself can be inferred from the float trajectory. Thus a single float trajectory becomes representative of a huge mass of water which is being advected by the eddy, and may have particular water property characteristics – for example, high salt and high temperature in the case of Mediterranean Water eddies, or Meddies (ARMI, HEBERT, OAKEY, PRICE, RICHARDSON, ROSSBY and RUDDICK, 1989). This water is anomalous to water surrounding the eddy as it drifts through the ocean. Thus float trajectories in discrete eddies reveal the paths of water mass anomalies. This, in turn, gives clues to ocean fluxes. Additional information obtained from the float trajectories includes the size of the eddies, their rotation rates, their swirl speeds, and how they change over time.

Information about eddies is important because energetic ones, like Gulf Stream rings, are thought to play a leading dynamical role in the general circulation. The behavior of eddies gives important clues to the sources and sinks of energy and shows how the ocean works.

Float data have been recently used to map statistical properties of the velocity field in the North Atlantic (OWENS, 1991). Maps of eddy kinetic energy show a large peak in the vicinity of the Gulf Stream, as well as other geographical patterns. The maxima in eddy energy seem to coincide with looping trajectories, but the connection is not obvious, because individual trajectories are highly convoluted. Consequently, summary plots of trajectories are so complicated that any patterns are difficult to see even with a practiced eye.

The present analysis separates trajectories which are clearly looping from nonlooping in order to learn about eddy motions in the eddy energy peak in the Gulf Stream as well as elsewhere along the western boundary and in the interior of the ocean. Studies of discrete eddies should lead to a broader understanding not only of mesoscale oceanographic processes, but also of the circulation and structure of the ocean as a whole.

This introduction is followed by a description of the float data and the methods used to identify loopers. Next is an overview of the general characteristics of the loopers and inferred eddies, including their geographical distribution, swirl velocity, temperature, translation velocity, and eddy kinetic energy. There follows a more detailed discussion of the loopers in three regions: the western North Atlantic, the Newfoundland Basin, and the eastern Atlantic. The western North Atlantic is subdivided into the Gulf Stream, the western boundary region south of 30°N, and the Sargasso Sea. The trajectories and formation of anticyclones south of the Gulf Stream are discussed at some length. The main results are reiterated in the final summary.

2. DATA

The U.S. SOFAR float data set consists of 230 individual trajectories amounting to 240 float years (Table 1, Fig. 1). The trajectories have been collected over the last 18 years, but mostly within the last 5-10 years. The early data (1972-1982) were obtained by T. Rossby at the University of Rhode Island, and the more recent data (1980-1989) by B. Owens, J. Price, P. Richardson and W. Schmitz at the Woods Hole Oceanographic Institution. Before 1980 tracking was primarily by means of shorebased listening stations; afterwards moored listening stations were used. Details of the individual experiments and data have been published in a series of data reports and papers (see Table 1) and the data and velocity statistics have been summarized by OWENS (1991).

Most floats were ballasted to drift at one of three nominal depths: shallow, around 700m; mid-depth, nominally 1300m but ranging from 1100-1500m; and deep, or around 2000m. Float data are so grouped in this paper. Trajectories at 700m are most numerous and provide the most comprehensive coverage of the western North Atlantic. Most trajectories in the Gulf Stream, its recirculation, and the Newfoundland Basin were at 700m. Mid-depth trajectories are divided into two main groups – one near 30°N, 70°W; the other in the eastern Atlantic where floats were deployed in the Mediterranean Water near 1100m. Most trajectories at 2000m are from the Gulf Stream and recirculation to the south. A few 2000m trajectories are from the southwestern region and the Newfoundland Basin. It is important to keep this inhomogeneous coverage of the available float data in mind when comparing summaries of different regions.

TABLE 1. Summary of SOFAR Float Experiments

Experiment[a]	Years	Approximate Location	Number of Floats	Depths (m)	Average Duration Days	Looper Days	Total Float Days	Float Days	References[b]
MODE 9MO)	1972-76	28°N 70°W	47	1500	178	366	8,360	22.9	3,4,7,11,19, 21,22,28
Ring (RI)	1974-75	33°N 70°W	8	1100	154	252	1,228	3.4	2,11
PreLDE (PL)	1975-79	20-30°N, 55-75°W	20	700,2000	586	1,066	11,722	32.1	6,7,8,11,20, 22,27
LDE (LD)	1978-79	31°N 70°W	45	700,1300	164	1,509	7,364	20.2	7,11,12,22 23,27,28
LR/GS	1978-79	36°N 65°W	5	700,1300,2000	316	0	1,582	4.3	11,25,27
GUSREX (GU)	1980-85	24-42°N 55°W	39	700,200	563	2,375	21,940	60.1	5,9,11,15,16, 17,24,29
Site L (SL)	1982-85	34°N 70°W	21	700	424	2,026	8,898	24.4	11,14
Eastern Basin (EB)	1984-88	32°N 24°W	32	110	698	3,933	22,350	61.2	1,13,18,26, 29,31,32
Newfoundland Basin (NB)	1986-89	45°N 40°W	13	700,1200,2000	333	1,414	4,334	11.9	10,11
Summary	1972-89		230	700-2000	381	12,941	87,778	240.3	

[a] Two letters which refer to the experiment plus a number are used to identify individual floats. MODE stands for the Mid-Ocean Dynamics Experiment, Ring refers to an experiment to track Gulf Stream rings, LDE stands for the Local Dynamics Experiment of Polymode, LR was a test of long range float tracking, GS was a test of float tracking in the Gulf Stream, GUSREX stands for the Gulf Stream Recirculation Experiment, and Site L refers to a location near 34°N 70°W where floats were launched in clusters.

[b] References

1. ARMI *et al* (1989)
2. CHENEY *et al* (1976)
3. DOW *et al* (1977)
4. FREELAND *et al* (1975)
5. KENNELLY and McKEE (1984)
6. McDOWELL and ROSSBY (1978)
7. McKEE (1986)
8. O'GARA *et al* (1982)
9. OWENS (1984)
10. OWENS and ZEMANOVIC (1990)
11. OWENS (1991)
12. PRICE and ROSSBY (1982)
13. PRICE *et al* (1986)
14. PRICE *et al* (1987)
15. RICHARDSON (1983)
16. RICHARDSON (1985)
17. RICHARDSON *et al* (1981)
18. RICHARDSON *et al* (1989)
19. RISER *et al* (1978)
20. RISER and ROSSBY (1983)
21. ROSSBY *et al* (1975)
22. ROSSBY *et al* (1983)
23. ROSSBY *et al* (1986)
24. SCHMITZ (1985)
25. SCHMITZ *et al* (1981)
26. SCHMITZ *et al* (1988)
27. SHAW and ROSSBY (1984)
28. SPAIN *et al* (1980)
29. SPALL (1992)
30. WOODING *et al* (1989)
31. ZEMANOVIC *et al* (1988)
32. ZEMANOVIC *et al* (1990)

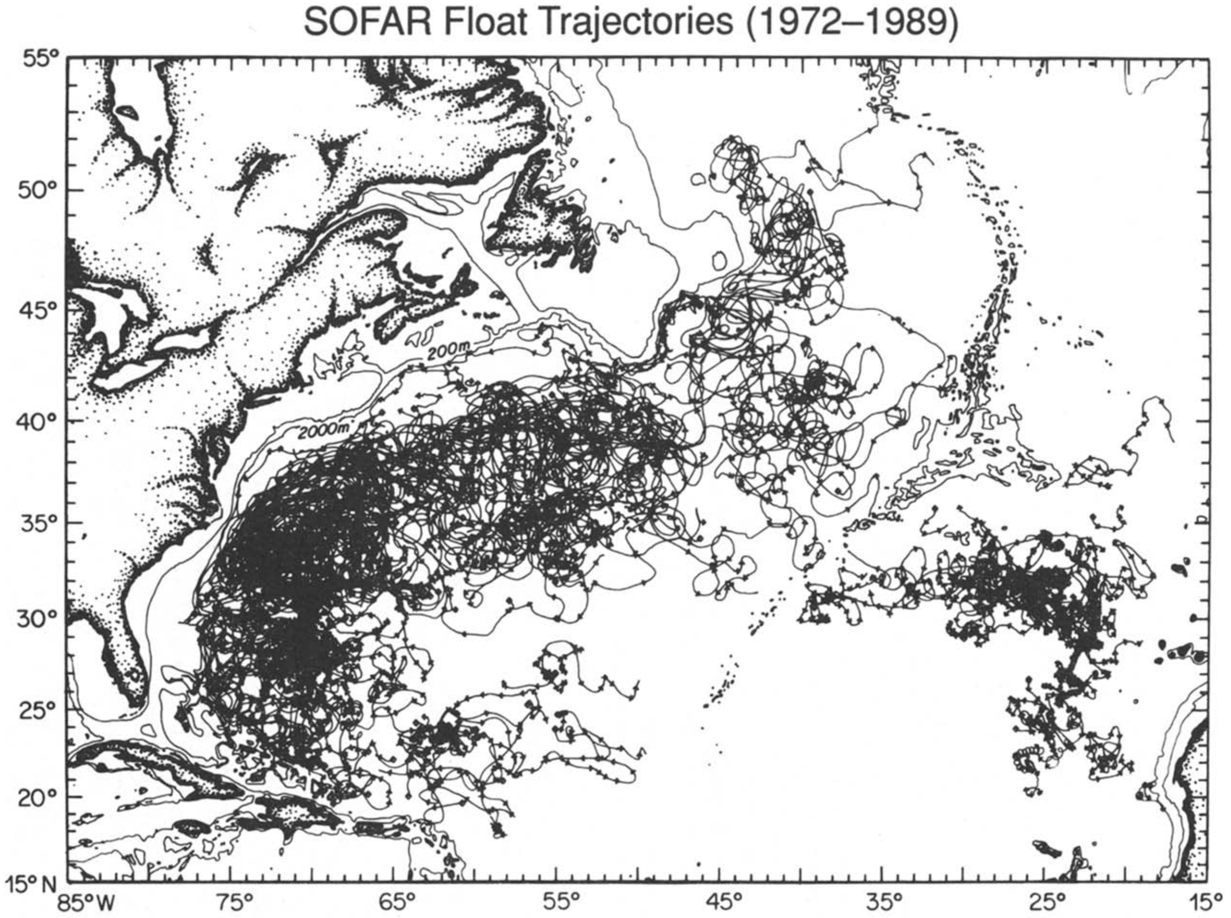

FIG.1. Summary of all SOFAR float trajectories in the North Atlantic. Two hundred thirty trajectories consisting of 240 float years of data were measured from 1972-1989. Arrowheads are spaced at 30-day intervals along trajectories. Trajectories are clustered at three main depths: at 700m throughout the Western Basin, at 1300m (1100m-1500m) near 30°N 70°W and in the Eastern Basin, and at 2000m predominantly in the Gulf Stream and recirculation. Convoluted trajectories show time variation of ocean currents.

3. METHODS

Each trajectory was visually examined for loops and cusps revealing the characteristic motion of particles in eddies – a rotational velocity around the eddy center, plus its translation. Some good examples of looping trajectories are shown in Figs 2, 3 and 4. Time series of velocity, temperature, and pressure have also been studied to help estimate when a float entered and exited an eddy. Many long trajectories in rings and Meddies, previously documented by shipboard measurements, provided guidance. Additional guidance was provided by H. Stommel's model of vortices, which shows trajectories of both active model vortices and passively advected model floats. SOFAR float trajectories reveal some of the same complex patterns as model ones.

Many SOFAR floats interpreted as being in discrete eddies significantly changed their looping rotation rate, radius, and the inferred eddy translation velocity over the course of a series of loops. A few trajectories displayed smallish loops embedded in larger ones, consistent with what might be obtained from a rotating elliptical or peanut-shaped eddy. Identifying trajectories as being involved in eddies was clearly subjective, and the possibility remains that the character of some trajectories may have been mis-identified.

Once a looping float trajectory (looper) was identified, consisting of around two or more consecutive loops in the same direction, various summary statistics were calculated and used to estimate the characteristics of the eddies. These results are listed in the Appendix. The number of loops was estimated visually and used to calculate the period of rotation (T). Average temperature and pressure were calculated. The mean translation rate of the eddy (V) was estimated by calculating the mean velocity of each float. The characteristic swirl velocity (V_θ) was estimated as being equal to the root mean square (RMS) velocity of the float about its mean velocity. That is, $V_\theta = [\overline{u'^2} + \overline{v'^2}]^{1/2}$ where $u' = u - \overline{u}$, u is the velocity in the eastward direction, $\overline{u}$ is the average velocity, u' is thus the departure from the average velocity, and $\overline{u'^2}$ is the variance; similarly for v

FIG.2a. Trajectory of float SL124, which drifted from November 1, 1982, to August 29, 1985, a total of 999 days, in the vicinity of the Gulf Stream. This longest-lasting float of the Site L experiment looped for 656 days in 4-5 different eddies, the number depending on whether or not two of the sets of loops are in the same anticyclone. Two looper portions are inferred to be in cold core cyclonic Gulf Stream rings. The chronology of this float is as follows: it began by looping in an anticyclone for 74 days (looper no.37), which looks as if it interacted with a nearby cyclone. It then drifted southeastward and looped in a cyclone for 133 days (no.2). During a close encounter with an anticyclone (no.44) and possibly Bermuda, it was expelled from the cyclone. It drifted north and looped one and a half times around another cyclone. It returned south and was entrained into an anticyclone (no.35), the same one from which float SL142 was detrained (no.44), where it looped for 261 days. It drifted northward and passed through the current meter array of BANE *et al* (1989). It was entrained into the Gulf Stream and went 1800km eastward. Finally, it was expelled from the Stream and into a cyclone (no.1) for 188 days and translated westward.

FIG.2b. Trajectory of Site L float SL132 at 700m. This float looped in five different eddies, three cyclones and two anticyclones. Four of the eddies were just offshore of the Gulf Stream, one near Bermuda. The total of looping days was 306 out of a possible 888 days.

FIG.2c. Trajectory of GUSREX floats GU106 and GU102 at 700m. Looper no.19 was in a newly formed cold core Gulf Stream ring for 361 days, a cyclone record. The average swirl velocity was 21cm s^{-1}, the average diameter 79km, the average period of rotation 14 days, and the average translation velocity of the eddy 2.6cm s^{-1} toward 229°. Looper no.46 was in an anticyclonic warm core eddy for 152 days. The average swirl velocity was 25cm s^{-1}, the average diameter 155km, the average period of rotation 22 days, and the average translation velocity of the eddy 4.0cm s^{-1} toward 270°. Both of these eddies contained 700m and 2000m floats (Table 3).

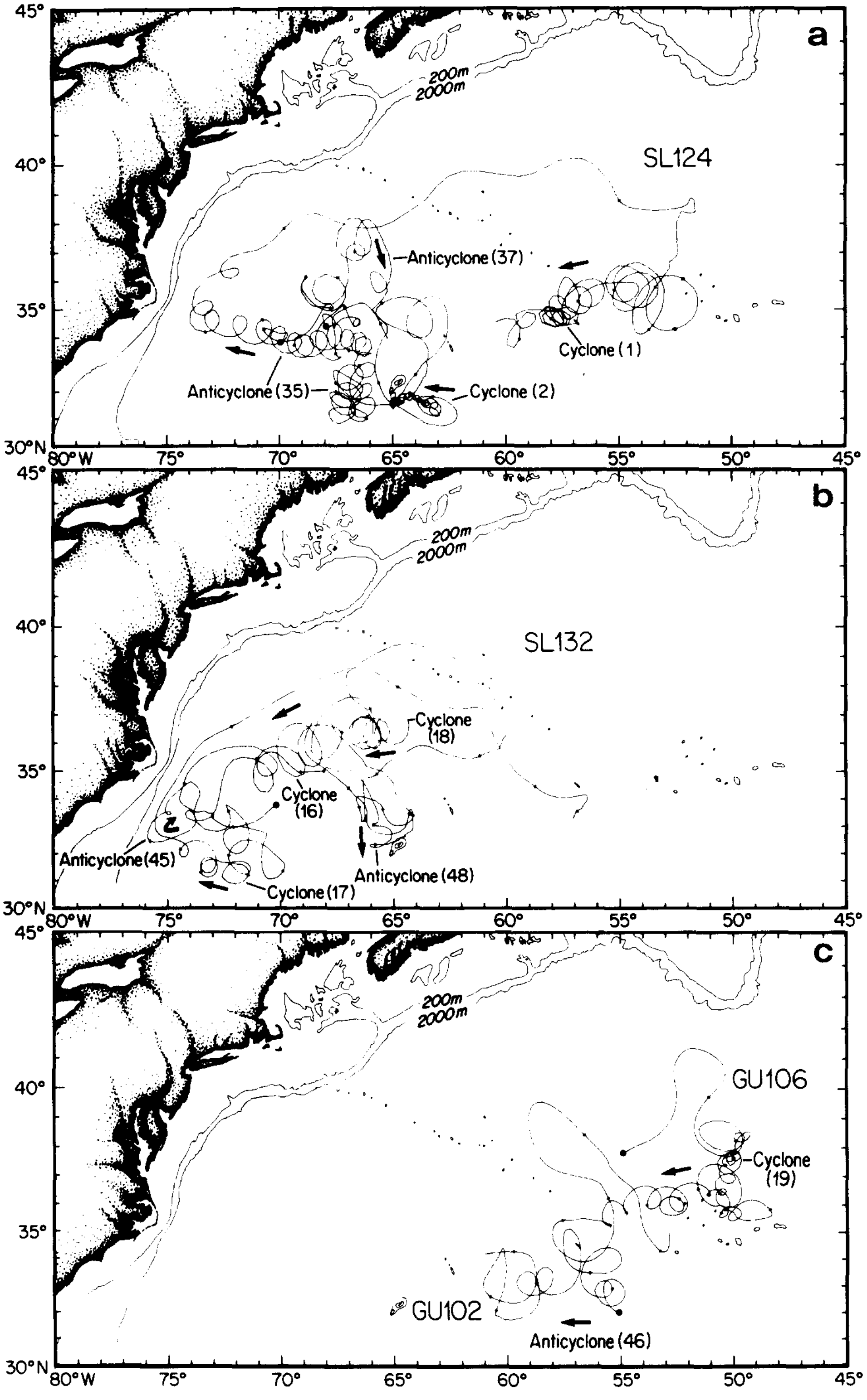
a
200m
2000m
SL124
Anticyclone (37)
Cyclone (1)
Anticyclone (35)
Cyclone (2)
b
200m
2000m
SL132
Cyclone (18)
Cyclone (16)
Anticyclone (45)
Cyclone (17)
Anticyclone (48)
c
200m
2000m
GU106
Cyclone (19)
GU102
Anticyclone (46)
45°
40°
35°
30°N
80°W
75°
70°
65°
60°
55°
50°
45°

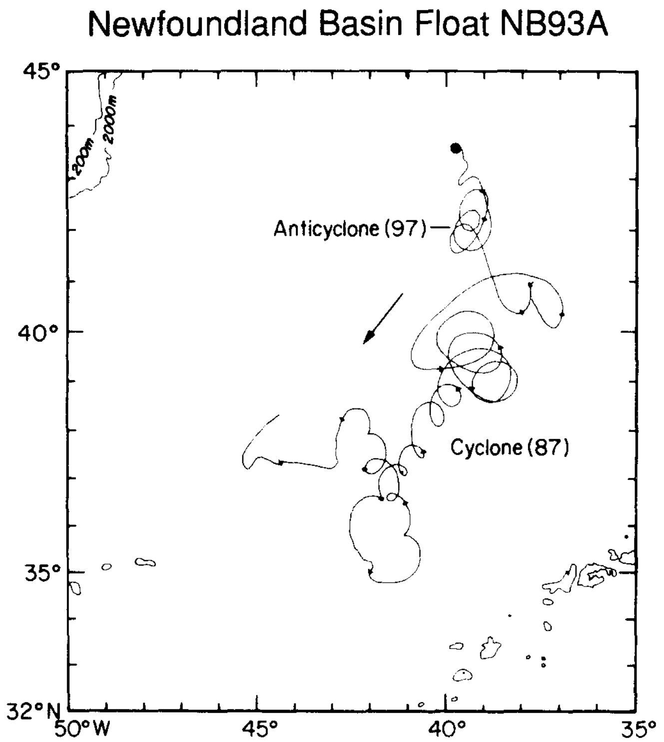

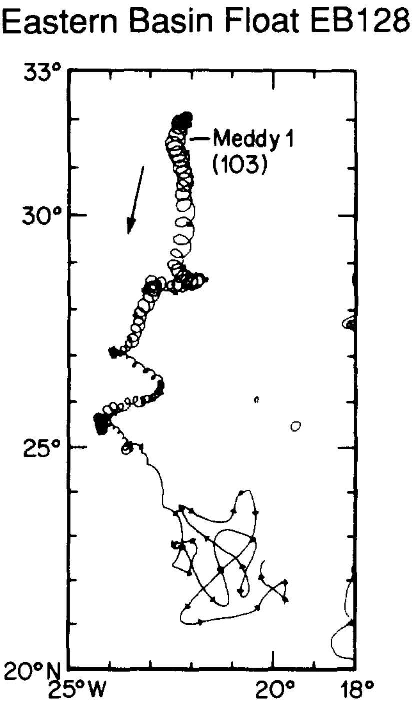

FIG.3. (above) Newfoundland Basin float NB93 at 700m. This float looped 15 times in a cyclonic eddy during 277 days (no.87). This longest looper in the Newfoundland Basin was located in the cluster of eddies near 40°N 40°W. The average swirl velocity was 16cm s^{-1}, the average diameter 84km, the average period of rotation 19 days, and the average translation velocity of the eddy 1.1cm s^{-1} toward 228°.

FIG.4. (left) Eastern Basin float EB128 and looper no.103 that set two records – the longest tracked looper at 821 days, and the most loops at 114. This float was deliberately launched in a Meddy. The trajectory clearly shows a change in characteristics near 24°N from a series of consecutive anticyclonic loops in the Meddy north of 24°N to more wave-like character after the float left the Meddy south of 24°N.

TABLE 2. Percentage of float days that are loopers

Experiment	Approximate Location	Total Float Years	Partition of data into depth ranges[a] All Depths Combined	700m	1100-1500m	2000m
MO	28°N 70°W	22.9	4.4 (100)		4.4 (100)	
RI	33°N 70°W	3.4	20.5 (100)[b]		20.5 (100)[b]	
PL	20-30°N 55-75°W	32.1	9.1 (46.6)	12.0 (38.6)		4.4 (82.6)
LD	31°N 70°W	20.2	20.5 (45.7)	23.5 (54.5)		17.5 (33.6)
LR/GS	36°N 65°W	4.3	0.0	0.0	0.0	0.0
GU	24-42°N 55°W	60.1	10.8 (76.8)	17.3 (78.7)		7.2 (74.1)
SL	34°N 70°W	24.4	22.8 (63.5)	22.8 (63.5)		
EB	32°N 24°W	61.2	16.9 (4.1)[c]		16.9 (4.1)[c]	
NB	45°N 40°W	11.9	32.6 (64.7)	47.4 (71.3)	17.6 (0)	0.0
Summary		240.3	14.7 (48.2)	20.7 (63.7)	13.8 (19.4)	6.2 (75.4)

[a] The first value in each column is the % of loopers calculated from the total number of looper days and the total possible float days at each depth. The second value, in parenthesis, is the % of these looper days that are cyclonic, or counterclockwise. Overall, 14.7% of the available float data are loopers consisting of two or more loops in the same direction. If loopers with three or more consecutive loops are considered, then the overall percentage of loopers decreases to 12.9%.

[b] These floats were deliberately launched in cyclonic Gulf Stream rings.

[c] Seven floats were deliberately launched in Meddies. If we exclude these loopers the values are 9.8% (7.6%) for the Eastern Basin.

in the northward direction. This calculated swirl velocity is a reasonable estimate of the looper swirl velocity for the case of a constant translation velocity. However, if a looper's translation velocity varies significantly over a series of loops, the calculated RMS velocity will tend to overestimate the swirl velocity. In general (but not always) the actual swirl velocity is significantly larger than the translation velocity, which suggests that the RMS velocity is a reasonable estimate for swirl velocity. In other calculations eddy kinetic energy (EKE) was estimated using $EKE = 1/2(\overline{u'^2 + v'^2})$. The mean diameter (D) of the loops was estimated from the mean period of rotation (T) and mean swirl velocity (V_θ) with the relation $D = V_\theta T/\pi$. Finally, the calculations include the translation velocity divided by swirl velocity, V/V_θ, and the Rossby Number R_0, which was estimated from $2V_\theta/fD$, which is equal to the inertial acceleration $2V_\theta^2/D$ divided by the Coriolis acceleration fV_θ.

Statistics for groups of loopers were calculated by two methods. In the first, averaging of individual loopers, each looper was considered to give an independent estimate of each quantity (V, V_θ, EKE, etc.). Quantities from loopers in certain regions were grouped and means calculated from the individual estimates. Standard errors of the mean were calculated from $[s/n]^{1/2}$, where s is the variance of a particular quantity about the mean and n is the number of individual loopers in the group. In the second method, averaging of bin data, original looper time series of daily values

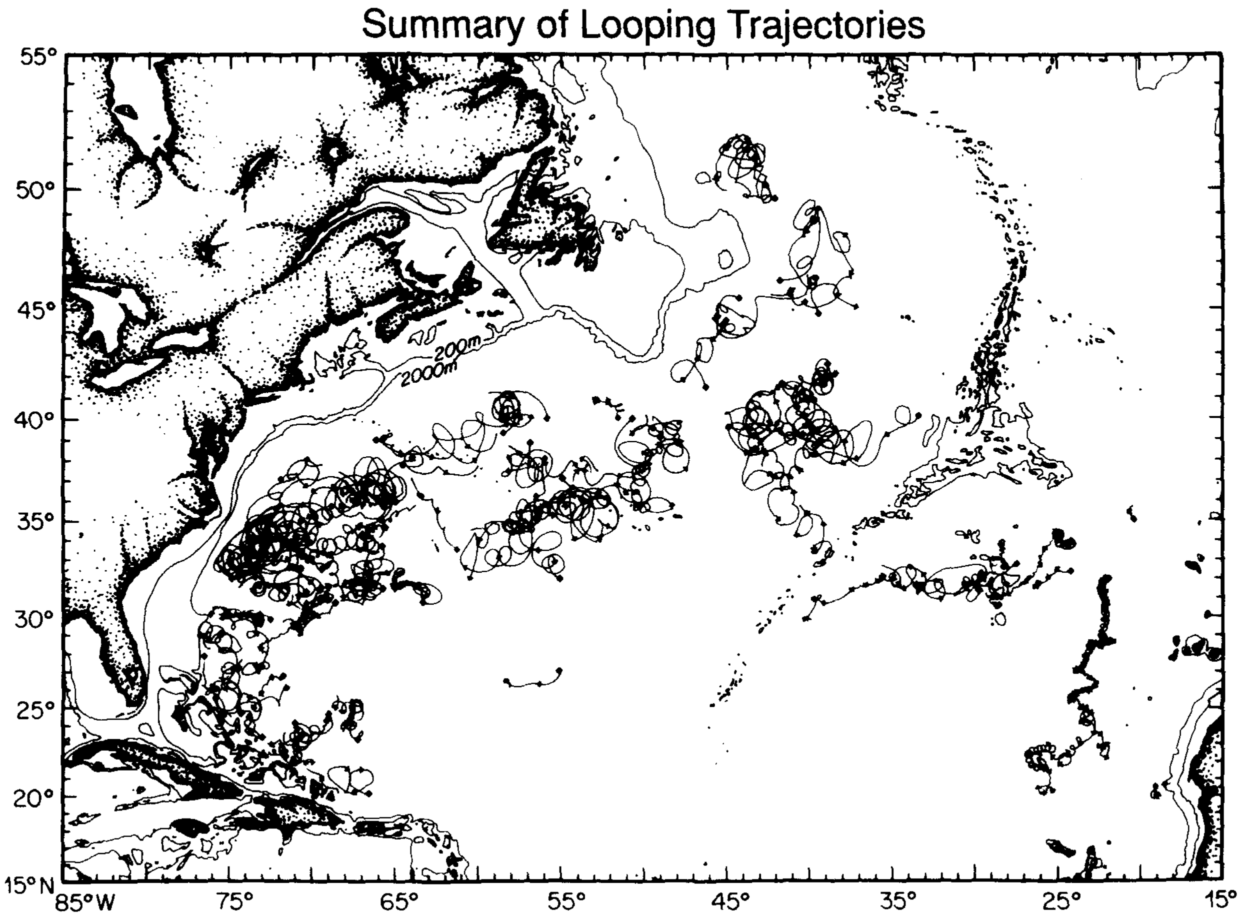

FIG.5. Summary of looping float trajectories that consist of two or more consecutive loops in the same direction, implying that the floats were trapped in discrete eddies. Most loopers (71%) in the western Atlantic are located at *700m. Overall, 21% of float data at 700m are loopers. The highest percentage is located in the Newfoundland Basin,* where almost half (41%) of the data are loopers, 71% of these rotating cyclonically (counterclockwise).

of u, v, temperature, and pressure were grouped in different space-depth bins and averages of these calculated. This allows a comparison of looper and nonlooper characteristics in the different regions. The second method evenly weighted daily values of each quantity, whereas the first method evenly weighted each looper. Standard error of velocity was estimated using $[2\tau s/N]^{1/2}$, where s is the variance of velocity about the mean velocity, N is the number of daily velocity observations, and τ is the integral time scale of the Lagrangian autocorrelation function, which was estimated to be 10 days for nonloopers. In practice, the number of degrees of freedom, N/τ, was estimated by summing the number of 10-day intervals for which each float was within a box (see OWENS, 1991). Since the average period of rotation of all loopers was 20 ± 1 days, the calculated standard error is approximately equal to $[s/\text{number of loops}]^{1/2}$.

4. PERCENTAGES OF LOOPERS

A total of 118 individual trajectories consisted of two or more loops (loopers) and were thus identified to be in discrete eddies (Fig.5, Table 2). The number of individual eddies was estimated to be 103 because on at least 16 occasions more than one float looped in the same eddy. Overall 35.4 float years of data or 15% of all available data were in loopers. Eliminating floats deliberately launched in Gulf Stream rings and Meddies decreases the percentage of loopers to 13%. However, 14 floats in the Eastern Basin were deliberately launched in a Meddy-free region, as determined by a shipboard survey before launch, so the 13% is probably a lower bound. If we assume that 14% is a representative average for the area encompassed by eddies, and that the average diameter of eddies is 80km (as estimated from the loopers), we find that the North Atlantic has a population of roughly 10^3 discrete eddies, with a characteristic spacing between centers of around 200km.

The available float data indicate that the distribution and type of eddies varies significantly from region to region. The highest percentage of loopers (percentage of recorded float days in loopers) occurred at a depth of 700m in the Newfoundland Basin and in and just south of the Gulf Stream. In the Newfoundland Basin almost half of recorded float days were in loopers. This is seen qualitatively in individual float trajectories there, with floats appearing to jump from one eddy to the next with little time between. In an extreme example, float NB99 drifted in the Newfoundland Basin for a total of 1032 days, of which 560 days were spent looping in what appear to be seven different eddies, the most sampled by any individual float. In the vicinity of the Gulf Stream the percentage of float days spent in loopers ranged from 17-24% (Table 2). Here also some floats were caught up successively in several different eddies – float SL132 looped in five different eddies for a total of 306 days, and float SL124 looped in possibly four different eddies for 656 days (Fig.2). South of the Gulf Stream recirculation, fewer loopers were seen except along the western boundary. In the region 20-30°N, 55-75°W, 12% of the daily data were loopers at 700m, as measured in the pre-Polymode Local Dynamics Experiment (pre-LDE). In the Eastern Basin, 17% of recorded float days at 1100m were loopers, but this value decreased to 10% when we excluded floats launched on purpose in Meddies.

The percentage of float days spent in loopers decreased significantly at increasing depth (Table 2). Qualitatively, far fewer deep trajectories loop than shallow ones. Overall, 21% of float days recorded at 700m were in loopers, compared to only 6% at 2000m. Both the experiments that contain significant amounts of 700m and 2000m data show this decrease: from 17% to 7% in GUSREX and from 12% to 4% in pre-LDE. A decrease is also seen from 24% at 700m to 18% at 1300m in the LDE and from 47% at 700m to 18% at 1200m in the Newfoundland Basin Experiment.

5. SWIRL VELOCITY AND TEMPERATURE

5.1 Vertical variations in swirl velocity

There are at least two possible explanations for the decrease in loopers below 700m in the western Atlantic. The first is that there are simply more eddies at 700m than at 1300m or at 2000m. The second is that roughly the same number of eddies extend over the 700-2000m range, but their swirl velocity is swifter at 700m so that deep floats do not make closed loops so often. Both explanations are probably partially correct, but supplemental data are needed to be definitive. The available data support the latter explanation in the vicinity of the Gulf Stream region, from where most 2000m float data comes. The average swirl velocity loopers between 35°N and the Gulf Stream (40°N) was 32(±3)cm s^{-1} at 700m and 12(±2)cm s^{-1} at 2000m. The average diameter of these loopers was 109 (±12)km at 700m and 88 (±6)km at 2000m. In three cases, floats at 700m and 2000m simultaneously looped in the same eddy – two cyclonic Gulf Stream rings and one anticyclone (Table 3). In all three cases, the deep floats looped once as the 700m looper floats passed overhead, and the rotation at 2000m was in the same direction as that at 700m. The swirl speeds at 700m versus 2000m were (1) 13.4cm s^{-1} vs 10.9cm s^{-1}; (2) 10.4cm s^{-1} vs 3.6cm s^{-1}; and (3) 25.1cm s^{-1} vs 9.1cm s^{-1} (Table 3). The average decrease in swirl velocity was (1) 19%, (2) 65% and (3) 64%. Since most shear is inferred to occur across the thermocline, with relatively little shear below 2000m, these values imply a deep penetration of swirl velocity underneath the eddies.

The documentation of an eddy with short vertical scales ~300m) in the LDE (RISER, OWENS, ROSSBY and EBBESMEYER, 1986) together with data from other submesoscale coherent vortices (DUGAN, MIED, MIGUEREY and SCHUETZ, 1982; McWILLIAMS, 1985) suggest that many small discrete eddies do not extend coherently from 700m to 2000m. Where our floats sampled these kinds of eddies, the explanation that there are more eddies at shallow depths is correct. Since most of our loopers had diameters larger than the 20km diameter of the eddy described by RISER *et al* (1986), most of the eddies in which these floats were looping were probably thicker than this eddy, but how thick is unknown.

5.2 Regional variations of swirl velocity

The swiftest swirl speeds, in excess of 40cm s^{-1} at 700m, were observed in cyclones near the Gulf Stream, and the anticyclones, with speeds of 35cm s^{-1} were not much slower. Newfoundland Basin eddies at 700m had an average swirl speed of 18cm s^{-1}, around half as swift as those near the Stream farther west. Eddies south of 30°N were slower (14cm s^{-1}) than these and smaller too, 82km versus 116km. Eastern Basin eddies were the slowest (6cm s^{-1}) and smallest (48km) of all. In the western Atlantic and Newfoundland Basin, the average swirl speeds of cyclones and anticyclones were similar.

5.3 Temperature variations in loopers

Cyclones were cooler than their background, implying a raised thermocline in their centers. Anticyclones were warmer, implying a depressed thermocline in their centers. This suggests a simple vertical structure with surface-intensified geostrophic current. However, if anticyclones are lens-shaped in the vertical, then not only could their upper parts be colder than the background temperatures but also their surface velocity could be lower than the maximum in the lens.

TABLE 3. Vertical variation of swirl velocity in eddies

Eddy	Lat	Long	Float ID	Number of Daily Observations	Pressure (db)	Temp (°C)	Swirl Velocity (cm s^{-1})	Diameter (km)
Cyclonic Ring 19	40°N	50°W	GU106	90	720	9.5	13.4	90
			GU155	82	2000	3.9	10.9	130
Cyclonic Ring 82	42°N	39°W	GU110	74	671	7.4	10.4	115
			GU159	74	2132	3.6	3.6	85
Anticyclone 46	32°N	55°W	GU102	31	744	12.7	25.1	200
			GU154	38	2130	–	9.1	105

Observations are from floats at 700m and 2000m (nominal) simultaneously looping in each eddy. In all three cases, the 2000m float looped once underneath the 700m looper. Values of pressure, temperature, and swirl velocity were estimated for the time interval when the shallow and deep floats were vertically aligned in each eddy. Diameter was estimated visually from the loops.

6. ROTATION DIRECTION

Roughly half of loopers (48%) observed were cyclonic, and half (52%) anticyclonic. However, there are great geographical differences in the number that rotate in a particular direction, as a result of the different eddy formation mechanisms. For example, in the Canary Basin almost all (96%) of the looper data at 1100m were anticyclonic, presumably because of the way eddies originate from the salty tongue of Mediterranean water emanating from the Straits of Gibraltar. Even when the loopers purposely launched in anticyclonic Meddies are excluded, 92% of the remaining Canary Basin loopers were anticyclonic. Cyclones predominate in and near the Gulf Stream and also in the Newfoundland Basin; 64% of Site L, 79% of GUSREX, and 71% of Newfoundland Basin 700m loopers are cyclonic. This can be interpreted as showing that (1) there are approximately two to three times more cyclones than anticyclones in these areas or (2) there are roughly similar numbers but that the cyclones have a swifter swirl velocity and therefore cause more float loops. However the eddy velocity statistics, although imperfect, show that the average swirl velocity of cyclones and anticyclones are similar, so we interpret the data as showing there to be two to three times more cyclones. Most of the floats were launched in and to the south of the Gulf Stream, and are inferred to have sampled cold core cyclonic Gulf Stream rings, which abound in the area. Many cyclonic float trajectories look similar to those of surface drifters in documented rings (RICHARDSON, 1980), and several cyclonic trajectories to the south of the Gulf Stream originated from meanders which were observed in satellite infrared images (see OWENS, 1984). Considering the density of cyclonic rings in the Sargasso Sea, it is surprising that equivalently strong anticyclones were seen. The formation and life history of these anticyclones is discussed later. Only two anticyclonic loopers (nos 38, 54) are inferred to be warm core rings north of the Gulf Stream (near 40°N). In the southwestern region, half (53%) of the loopers were cyclonic. Of the 19 LDE loopers, 46% were cyclonic, of the 14 pre-LDE loopers, 47% were cyclonic (52% if we exclude the two anticyclonic loopers from floats deliberately launched in a salty eddy as reported by McDOWELL and ROSSBY, 1978), and of the three MODE loopers, all were cyclonic (which seem to be anomalous).

7. EDDY KINETIC ENERGY

The EKE distribution of the North Atlantic at 700m based on float data is shown in Fig.6. The general trends are as follows:

1. high EKE along the Gulf Stream, with values reaching ~1000cm^{2}s^{-2} near 37°N 65°W, and extending into the Newfoundland Basin where values are 300-400cm^{2}s^{-2},
2. high values of 50-150cm^{2}s^{-2} along the western boundary (2000m depth contour) south of 30°N, and
3. a minimum of around 15cm^2 s^{-2} in the Sargasso Sea near 25°N 55°W.

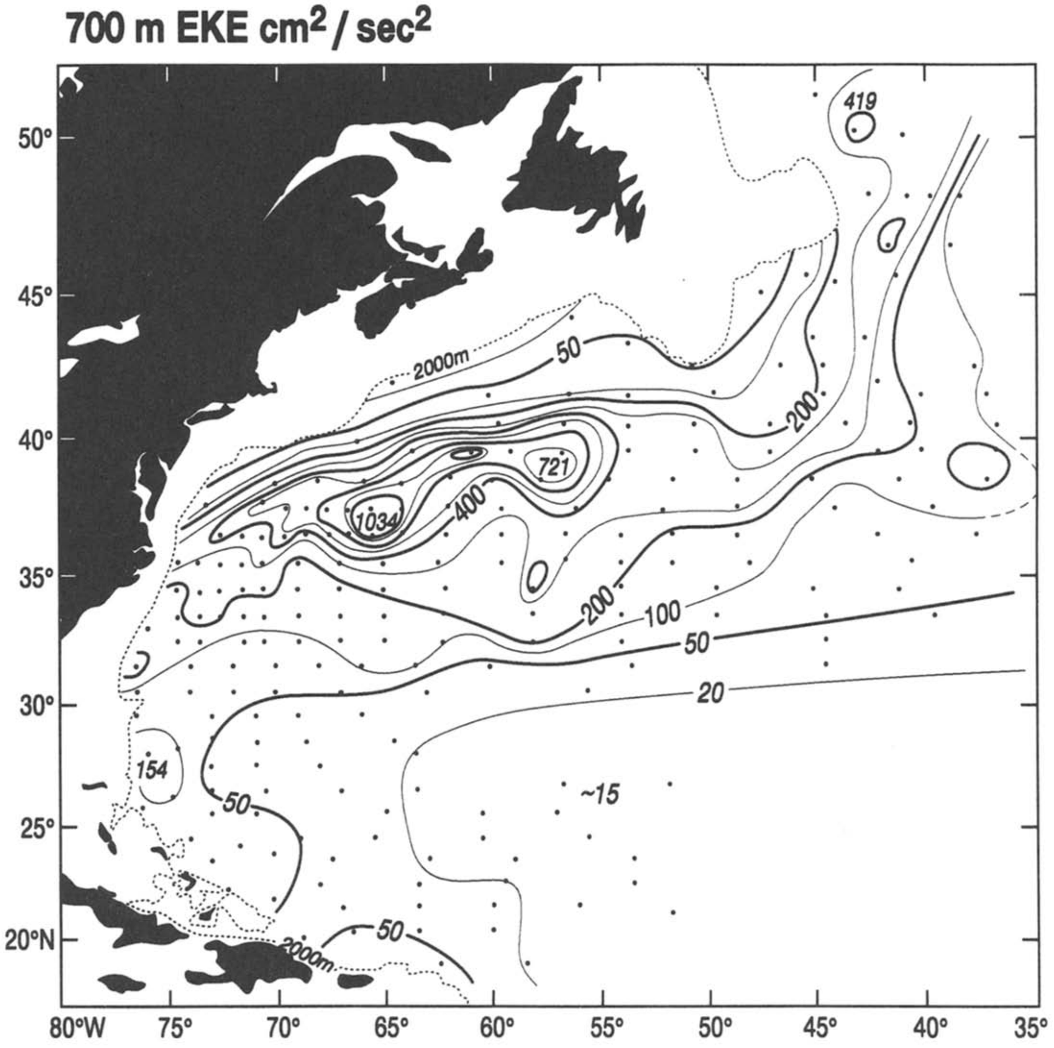

FIG.6. Eddy Kinetic Energy (EKE) distribution of the western North Atlantic based on all available 700m floats. Contours were drawn by hand based on the box averages calculated and shown by OWENS (1991, his Fig.8).

These values were calculated from all available floats. For specific regions, EKE was calculated from loopers and nonloopers separately in order to estimate the importance of loopers to this distribution. In general, loopers were significantly more energetic than nonloopers, which implies that the eddies are important dynamically. The most energetic loopers (Fig.7) were concentrated in the areas of high EKE shown in Fig.6, although a few energetic loopers were found south of the Stream in an area of lowish EKE into which presumably they had propagated. In the western Gulf Stream region (31°N-37°N, 65°W-75°W) at 700m, the EKE of loopers was 404cm^{2}s^{-2}, which is 2.7 times larger than EKE of 151cm^{2}s^{-2} from nonloopers, which included some Gulf Stream floats (Table 4). The EKE of cyclones was 408cm^{2}s^{-2}, indicating that on average they were equivalently energetic in this region. In this box, 17% of data are loopers, of which 50% are cyclones.

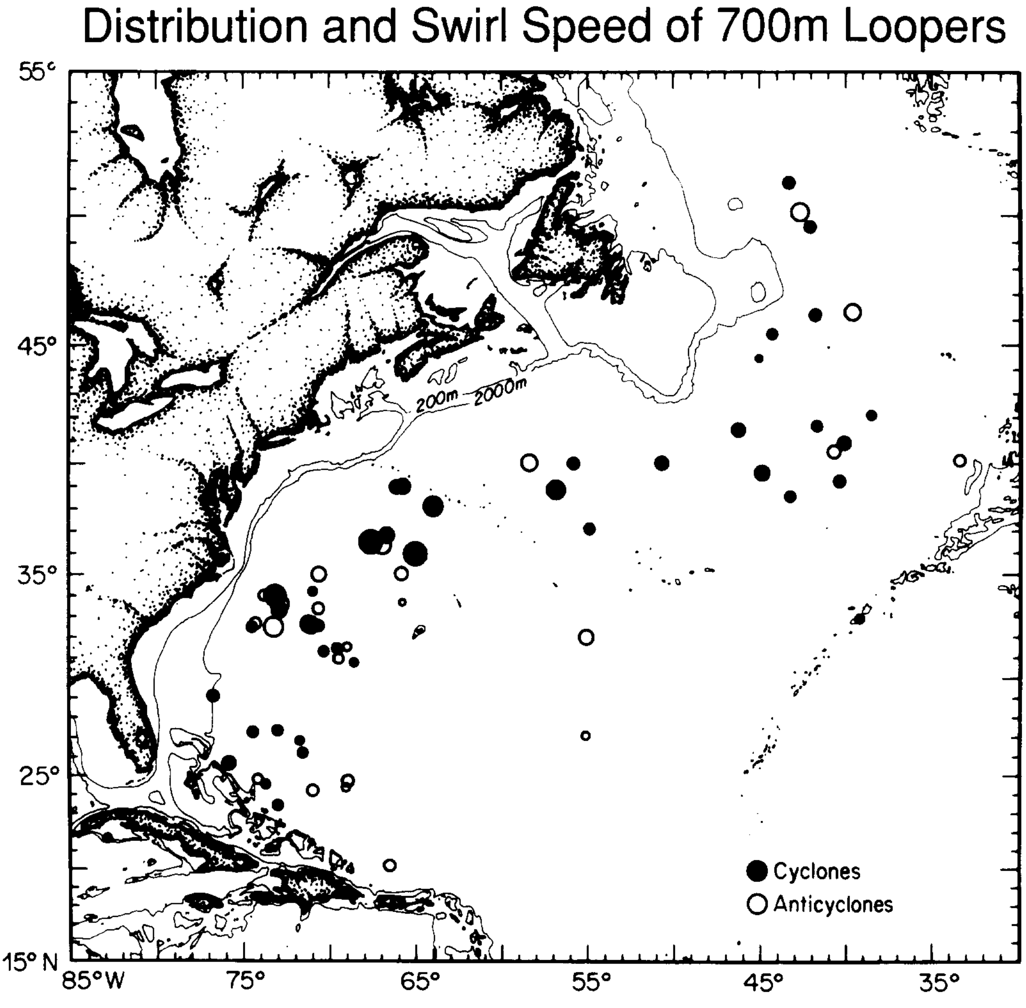

FIG.7. Distribution and swirl speed of 700m loopers (600m-800m). Each dot is placed at the first position of a looper. The diameter of each dot is proportional to swirl speed in 5cm s^{-1} increments. Largest swirl speeds are 47cm s^{-1} and 48cm s^{-1} in cyclonic Gulf Stream rings south of the Stream. Eddy kinetic energy of the loopers is proportional to the square of the swirl speed or area of the dot.

TABLE 4. Regional looper statistics

	Number of Observations	Ndf[a]	$\overline{u}$ (cm s^{-1})	$\overline{v}$ (cm s^{-1})	EKE (cm^2s^{-2})	$\overline{T}$ (°C)	$\overline{P}$ (db)
1. Western North Atlantic-Gulf Stream region at 700m (31-37°N, 65-75°W)							
All floats	6924	684	-0.62± 0.56	0.60 ± 0.53	204	12.99	734
Loopers	1180	122	-2.50 ± 2.58	-0.56 ± 2.57	404	13.10	710
Cyclonic loopers	589	62	-4.02± 3.54	-0.66 ± 3.71	408	12.61	705
Anticyclonic loopers	591	60	-0.98 ± 3.74	-0.47 ± 3.55	400	13.98	720
Nonloopers	5155	517	-0.31± 0.81	0.89 ± 0.72	151	12.97	738
2. Gulf Stream recirculation at 700m (29-35°N, 62-73°W; 32-37°N50-62°W)							
All 700 floats	8891	888	-1.74± 0.57	-0.60 ± 0.53	134	12.25	719
Loopers	2126	199	-2.26 ± 1.74	-0.35 ± 1.66	288	12.39	701
Nonloopers	6765	687	-1.59 ± 0.52	-0.69 ± 0.48	88	12.21	724
3. Western North Atlantic loopers west of 50°W, clear of Gulf Stream and western boundary (25-35°N, 50-70°W)							
All loopers	3810	350	-2.47 ± 1.19	-0.21 ± 1.18	245	10.60	949
Cyclones	2290	222	-2.59 ± 1.54	-0.34 ± 1.51	258	9.49	997
Anticyclones	1520	128	-2.30 ± 1.88	-0.02 ± 1.89	228	12.85	864
700m loopers	2697	242	-2.74 ± 1.64	-0.49 ± 1.61	320	12.17	708
1300m loopers	709	69	-2.02 ± 1.50	-0.17 ± 1.53	80	4.91	1318
2000m loopers	404	39	-1.46 ± 1.28	1.61 ± 1.67	44	3.62	2051
700m nonloopers	6505	641	-0.09 ± 0.31	-0.15 ± 0.30	58	12.18	696
1300m nonloopers	4821	483	-0.19 ± 0.17	-0.06 ± 0.20	17	4.80	1316
2000m nonloopers	3951	383	-0.62 ± 0.19	-0.05 ± 0.21	16	3.60	2055
4. Newfoundland Basin Cluster (33-43°N 35-45°W)							
All 700m floats	2338	225	0.74 ± 0.81	-0.66 ± 0.82	150	9.08	696
Loopers	1277	108	-0.64 ± 1.74	-0.91 ± 1.77	166	8.61	694
Cyclones	996	82	-0.17 ± 1.98	-0.62 ± 1.96	159	7.97	692
Anticyclones	281	26	-2.32 ± 3.59	-1.93 ± 4.03	190	10.85	701
Nonloopers	947	98	2.36 ± 1.62	-0.06 ± 1.63	129	9.67	698
5. Eastern Basin							
All	21267	1951	-0.28 ± 0.09	-0.15 ± 0.09	16	8.37	1108
Loopers	2524	235	-0.87 ± 0.72	-0.90 ± 0.72	61	9.15	1124
Loopers (no Meddies)	887	86	-1.67 ± 0.68	-0.19 ± 0.70	20	8.48	1110
All except Meddies	18578	1706	-0.25 ± 0.10	0.04 ± 0.10	8	8.16	1108
Nonloopers	17621	1623	-0.16 ± 0.09	0.05 ± 0.10	7	8.14	1108
All west of seamounts	2318	216	-0.81 ± 0.23	0.05 ± 0.22	10	8.04	1078
Loopers 112,113,114 west of seamounts	451	44	-2.74 ± 0.95	-0.68 ± 0.98	20	8.70	1094

[a] Ndf stand for Number of degrees of freedom and was estimated by summing the number of 10-day intervals for which each float was within a box.

An examination of individual loopers at 700m in this region throws more light on the averages. Eleven cyclones and four anticyclones began in the box. The three most energetic loopers were cyclones that look like cold core Gulf Stream rings; EKE values of these three ranged from 959 to 1162cm^{2}s^{-2}, almost twice as energetic as the three most energetic anticyclones, (582-648cm^{2}s^{-2}). These extreme values are in sharp contrast with the averages possibly because (1) several weak cyclones significantly lowered the average cyclone EKE, and (2) a single energetic anticyclone was tracked for a long time (430 days) with two floats (nos 35 and 44); this anticyclone which may not have been representative strongly influenced the long term average.

In the Sargasso Sea west of 50°W and clear of the Stream and western boundary, the EKE of loopers declined strongly from 320cm^{2}s^{-2} at 700m to 80cm^{2}s^{-2} at 1300m, and to 44cm^{2}s^{-2} at 2000m. EKE values of nonloopers grouped in a box 25°N-35°N, 50°W-70°W showed a similar decline of 58cm^{2}s^{-2} at 700m to 17cm^{2}s^{-2} at 1300m, and 16cm^{2}s^{-2} at 2000m. This suggests that loopers were around five times more energetic than background floats. However, these values are averages over a region in which there is a significant meridional gradient in EKE in both nonloopers and loopers (Fig.6), so the values are approximate.

In the Eastern Basin at 1100m, the EKE was 7.3cm^{2}s^{-2} for nonloopers and 61cm^{2}s^{-2} for loopers, a more than eight-fold increase. Meddy floats were the most energetic loopers, with an average EKE of 85cm^{2}s^{-2} and a maximum 151cm^{2}s^{-2} for no.108; the corresponding average EKE of nonmeddy loopers was 20cm^{2}s^{-2}.

Compared to these regions, in which loopers are clearly much more energetic than background floats, the Newfoundland Basin cluster of loopers (33°N-43°N, 35°W-45°W) is anomalous. Here the EKE of loopers was 166cm^{2}s^{-2}, greater but not statistically so at the 95% level of significance than the EKE of nonloopers, 129cm^{2}s^{-2}. The values for cyclones and anticyclones, 159cm^{2}s^{-2} and 190cm^{2}s^{-2} respectively, were not statistically different. The nearly uniform EKE distribution may be explained by the region being filled with closely packed eddies. In the Gulf Stream region, the Sargasso Sea, and especially the Eastern Basin, locally energetic eddies appear to be embedded in a much weaker background flow.

8. TRAJECTORIES

Trajectories of eddies were estimated from the series of individual loops. Eddies generally drifted westward to southwestward at a rate of a few kilometers per day (Tables 5 and 6). This is true for eddies in the Eastern Basin (average velocity 1.1cm s^{-1} toward 254°), in the interior Newfoundland Basin (1.4cm s^{-1} toward 215°), and south of the Gulf Stream (2.8cm s^{-1} toward 262°). Both cyclones and anticyclones had similar kinds of trajectories and average velocities (within standard errors). An exceptional area was in or very close to the Stream and its northward extension in the Newfoundland Basin, where eddies appear to have been advected downstream in the Stream. A second exceptional area was close to the western boundary (south of 31°N), where 700m eddies tended to drift northwestward and 1300m and 2000m eddies drifted southeastward; again these are inferred to have been advected by boundary currents.

Table 5. Looper translation velocity

	$\overline{u}$ (cm s^{-1})	$\overline{v}$ (cm s^{-1})	Diameter (km)	Speed (cm s^{-1})	Direction (°T)
a. Sargasso Sea (west of 50°W, clear of Gulf Stream and western boundary)					
39 loopers	-2.80 ± .42	-0.38 ± .36	88 ± 8	2.83	262
24 cyclones	-2.97 ± .54	-0.38 ± .41	85 ± 9	2.99	263
15 anticyclones	-2.54 ± .67	-0.39 ± .67	93 ± 16	2.57	261
30 700m loopers	-3.14 ± .52	-0.74 ± .39	96 ± 10	3.23	257
5 1300m loopers	-1.72 ± .39	-0.22 ± .54	55 ± 11	1.73	263
4 2000m loopers	-1.64 ± .82	2.05 ± 1.48	66 ± 9	2.63	321
b. Newfoundland Basin (cluster near 40°N 40°W)					
10 loopers	-0.78 ± .52	-1.11 ± .50	116 ± 12	1.36	215
7 cyclones	-0.24 ± .53	-0.57 ± .60	116 ± 17	0.62	203
3 anticyclones	-2.04 ± .95	-2.37 ± .61	117 ± 16	3.13	221
c. Eastern Basin (110m)					
13 loopers	-1.03 ± .35	-0.29 ± .40	32 ± 10	1.07	254
3 Meddies	-0.74 ± .54	-1.28 ± .16	25 ± 1	1.48	210
3 anticyclones	-2.60 ± .60	-0.80 ± .21	48 ± 14	2.72	253

Average velocities were calculated from velocities of individual loopers. Duplicate, and shorter, loopers in the same eddy were omitted.

TABLE 6. Average characteristics of 700m cyclones and anticyclones in the Western North Atlantic

Latitude Band	30°N - Gulf Stream		20°N - 30°N	
Eddy Type	Anticyclones	Cyclones	Anticyclones	Cyclones
Number of loopers	15	22	5	7
Total number of days	1266 (38%)	2086 (62%)	497 (50%)	490 (50%)
Float duration (d)	84 ± 18	95 ± 15	99 ± 22	70 ± 12
Number of loops	6.9 ± 1.9	6.6 ± 1.5	4.9 ± 2.2	3.6 ± 0.6
Pressure (db)	729 ± 11	688 ± 12	746 ± 41	694 ± 2
Period of rotation (d)	16.2 ± 2.5	18.6 ± 1.9	28.0 ± 7.5	19.5 ± 2.1
Swirl speed (cm s^{-1})	-24.2 ± 2.4	25.3 ± 2.7	-13.5 ± 3.1	14.1 ± 1.9
Diameter (km)	100 ± 14	109 ± 9	92 ± 24	76 ± 14
700m Temperature (°C)	15.0 ± 0.3	10.7 ± 0.7	11.2 ± 0.4	11.9 ± 0.2

Average values were calculated by grouping individual loopers listed in the appendix.

9. WESTERN NORTH ATLANTIC

9.1 Gulf Stream region

The fastest swirl velocities were recorded near 700m in what look like cyclonic cold-core Gulf Stream rings. The four highest speeds ranged from 42-48cm s^{-1} (looper numbers 1, 8, 16, 18 – see the Appendix), in cyclones of average diameter 130 ± 10km. The highest swirl velocities in anticyclones near the Stream at 700m were somewhat less, 35-37cm s^{-1} (nos. 35, 37, 41, 45), and their average diameter was 107 ± 1km. Note that these anticyclones were found south of the Gulf Stream and thus are not Gulf Stream rings, which are cyclonic there.

The average swirl velocity of 700m loopers in the western North Atlantic from the Stream to 30°N was 25 ± 2cm s^{-1} (Table 6). The average for cyclones (25 ± 3cm s^{-1}) was not significantly different from that for anticyclones (24 ± 2cm s^{-1}). These average values are only rough estimates because swirl velocity is a function of diameter and because the sampling of diameters in cyclones and anticyclones may not have been equal.

To compare the temperatures of eddies, their temperatures were corrected to 700m using an assumed ambient vertical temperature gradient of 1°C/50m (Table 6). Between 30°N and the Gulf Stream, cyclones (10.7°C) were 4.3°C colder than anticyclones (15.0°C). Bin averages of temperatures in the vicinity of the Gulf Stream (31°-37°N, 65°-75°W) showed (a) an average difference between cyclones and anticyclones of 1.7°C, (b) that cyclones were 1.0°C colder than background water as measured by nonlooper floats, and (c) that anticyclones were 0.7°C warmer than background water. The temperatures imply a raised thermocline in cyclones and a depressed thermocline in anticyclones.

North of 30°N, eddies near the Gulf Stream were often advected downstream, but the pattern there was complicated by large amplitude meanders and complex interactions between eddies and the Stream (Fig.8). In a band southeast of Cape Hatteras between 31°-34°N, approximately nine eddies translated westward toward the Stream, where they made a sharp right hand turn as they coalesced with it. Approximately 13 different eddies, both cyclones and anticyclones, were advected downstream. Translation rates were quite fast, with speeds up to 15-20cm s^{-1}. The general motion of eddies near the Stream seems to be similar to that observed for cold-core cyclonic Gulf Stream rings tracked with surface drifters. These rings near the Gulf Stream tend to translate eastward when attached to the Gulf Stream, southward as they separate from the Stream, westward when they are free of the Stream, and northward when they begin an interaction with the Stream (RICHARDSON, 1983). Interactions with the Gulf Stream can be intense; some can be "fatal", when a ring completely coalesces with the Stream; others "nonfatal", when a ring separates from the Stream again, albeit often significantly modified. In general, floats in the present study did not remain in eddies long enough to completely resolve their interactions with the Stream.

Because the motion of floats is similar to surface drifters in documented rings, most cyclonic loopers near the Stream are inferred to be in cyclonic rings. The formation of one of the rings (no. 19) tracked by floats was confirmed with satellite infrared images and surface drifters (OWENS, 1984), but existence of other rings remains unconfirmed. The documented simultaneous presence of numerous Gulf Stream rings in that region (RICHARDSON, CHENEY and WORTHINGTON, 1978) provides circumstantial evidence that many cyclonic loopers are rings.

The longest recorded cyclonic looper in this region, no. 19, at 361 days was in a cold-core ring that formed near 38.5°N 50.5°W (Fig.2; see OWENS, 1984). In May 1980, a surface drifter in the Stream meandered southward near this spot. During the latter part of May, float GU106 meandered south from the Stream and in June began to loop. The simplest interpretation is that this ring formed

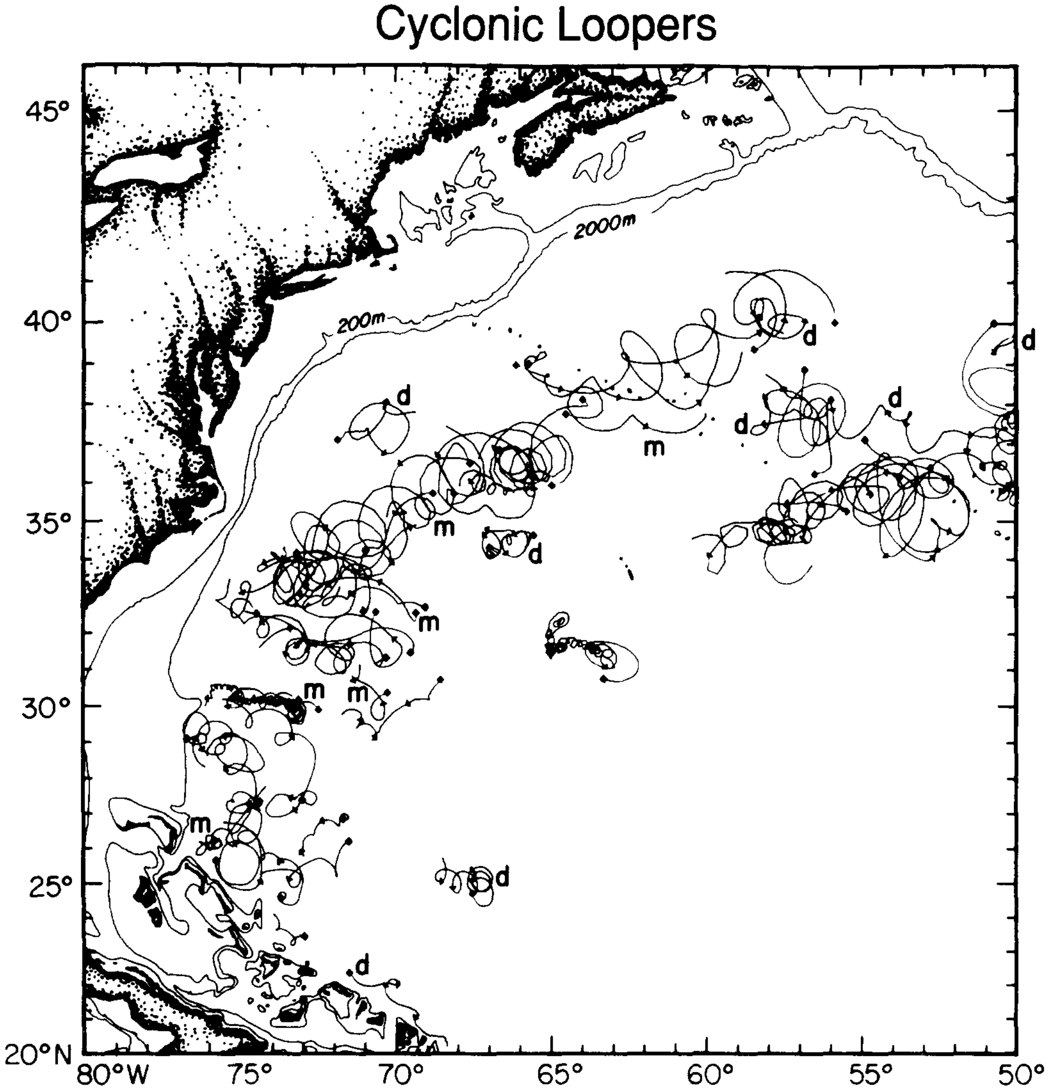

FIG.8. (A) Western North Atlantic cyclonic loopers.

during May-June, however it could have formed earlier and have been interacting with the Stream at that time. Prior to 7th June the region was cloudy, but afterwards infrared images show the ring for several months (J. Clark and P. LaViolette, personal communications). In July another float, GU104, meandered south from the Stream, in August GU104 looped once around the ring, suggesting it could have been partially connected to the Stream at that point. Looper no.19 (GU106) shows that the ring translated south to 36°N 49°W, then 660km westward along 36°N to 56.5°W. There, it presumably coalesced with the Stream, as suggested by the float's being entrained into the Stream. Another clear sample of a cold ring in this region was measured by looper no.1 for 188 days as it translated from 52.5°W to 60°W (690km) along 35°N (Fig.2).

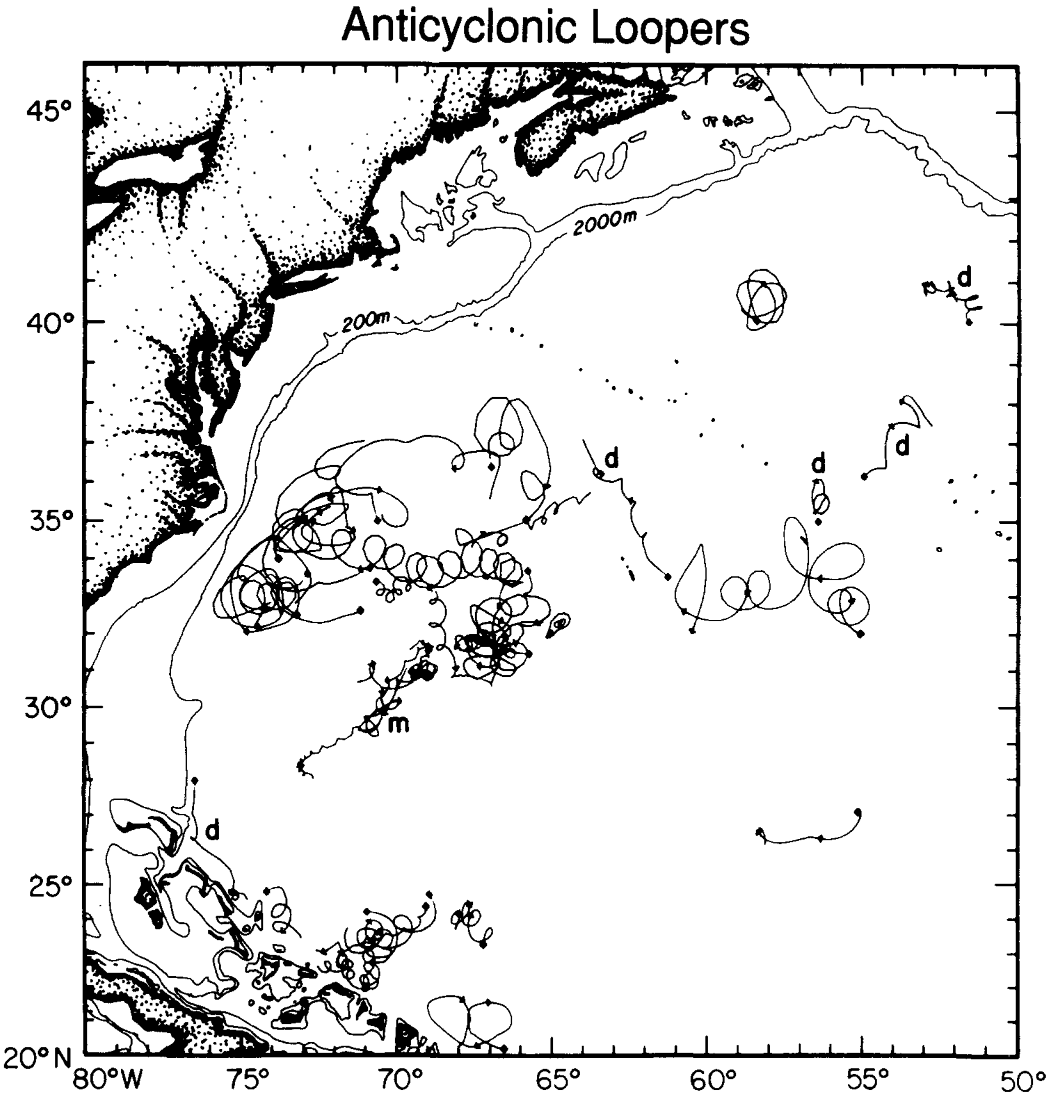

FIG.8(B) Western North Atlantic anticyclonic loopers.

9.1.1. Gulf Stream anticyclones. From the perspective of surface drifter trajectories, it is surprising to see the large number of anticyclones south of the Stream, because very few surface drifters looped anticyclonically in the region. The three that looped near 34°N 58°W were in two warm-core eddies generated in the vicinity of the Corner Seamounts near 36°N 52°W (see Fig.8C). A possible explanation is that anticyclonic eddies tend to have a lower swirl velocity near the surface than at 700m. In addition, many (though certainly not all) drifters were deliberately launched in cyclonic rings, which could have biased the data.

One of the longest float trajectories in an anticyclone (no.46) looped for 152 days as it translated 550km westward along 33°N from 55°W to 61°W (Figs 2C, 8B). An XBT and CTD section observed .t the time the float was launched showed this eddy to have a deep (>2000m) warm core

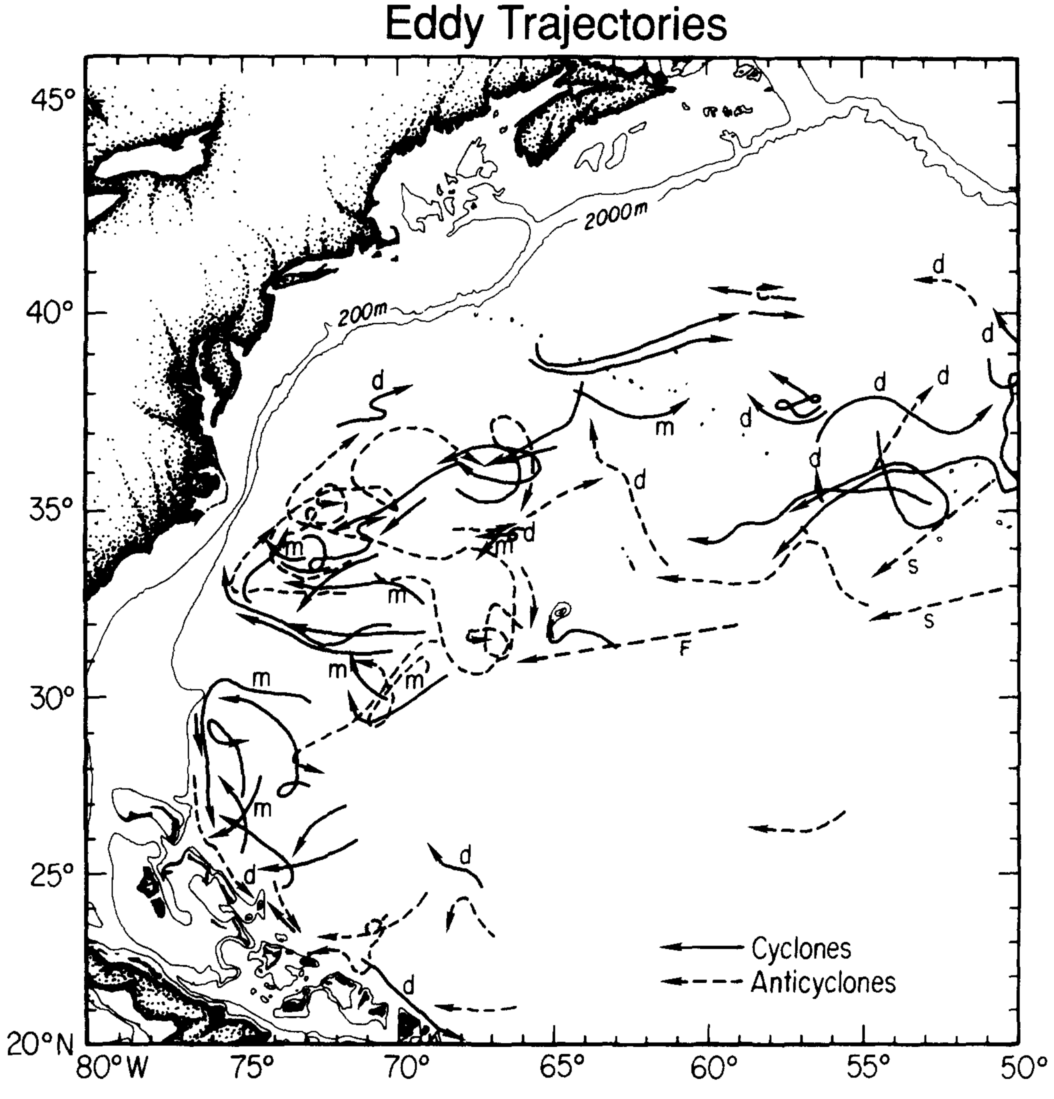

FIG.8(C) Trajectories of eddies inferred from loopers. Solid lines represent the path of cyclones, dashed anticyclones. S indicates two anticyclones tracked by surface drifters (RICHARDSON, 1980), F stands for a 700m French float that looped in an anticyclone (M. Ollitrault, personal communication), m is mid-depth or nominally 1300m, and d is deep or nominally 2000m. Eddies in this region generally translated westward at a few cm s^{-1}. Exceptions are in the Gulf Stream, where 13 eddies were advected downstream at speeds up to 15-20cm s^{-1}, and along the western boundary between 20°N and 30°N where 700m eddies tended to translate northwestward and 1300-2000m ones tended to translate southeastward.

with the thermocline depressed ~150m deeper in the center than nearby (KENNELLY and McKEE, 1984). This is probably an underestimate since the section was likely to have been off center. The proximity of this anticyclone to the two earlier ones tracked by surface drifters and the similar characteristics of the three eddies suggest that they all could have originated near the Corner

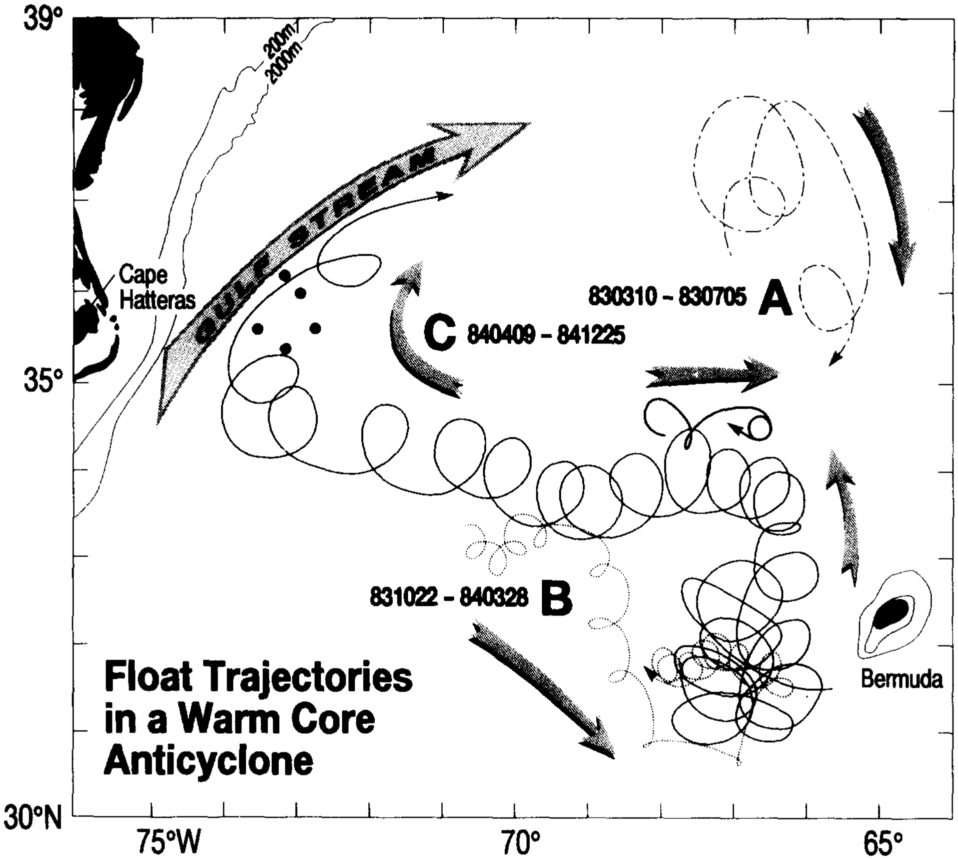

FIG.9. (A) Tracks of two floats in a warm core anticyclone.

Seamounts. A rather similar trajectory of an anticyclone was measured by a 700m French float in the same general area (M. Ollitrault, personal communication, Fig.8C).

The longest trajectory of an anticyclone was 430 days, obtained by combining data from two loopers (nos 35 and 44, Fig.9). Although there was an 11 day gap between the loopers, their close proximity, similar period of rotation and swirl speed before and after the gap strongly suggest that they were in the same eddy. The eddy trajectory might have been as long as 656 days if an earlier looper (no.37) was in the same eddy. Although the looping characteristics are similar, the 108 day gap makes the interpretation that a single eddy was responsible for the loopers tentative.

If we include this earlier looper, then the anticyclone began near the Gulf Stream near 37°N 67°W on March 10, 1983 (Fig.9). It translated southwestward to 34.5°N 66.5°W, where looper no.37 stopped. Looper no.44 began near 33°N 70°W on October 22, 1983, from where, the eddy translated southeastward, counter to the prevailing drift of the other eddies. It stalled and looped (2 cyclonic loops of the eddy center) near 31°N 67°W, then translated northwestward into the Stream near 36°N 73°W and finally downstream. As it was advected downstream, the eddy passed through a current meter array that recorded its characteristics. Thus, this anticyclone is noteworthy, not only for its long trajectory but also for its characteristics being so well documented. BANE, O'KEEFE and WATTS (1989) reported maximum swirl speeds greater than 50cm s^{-1} at a depth of 900m, a radius of 30km, and a temperature greater than 14°C and a maximum positive temperature

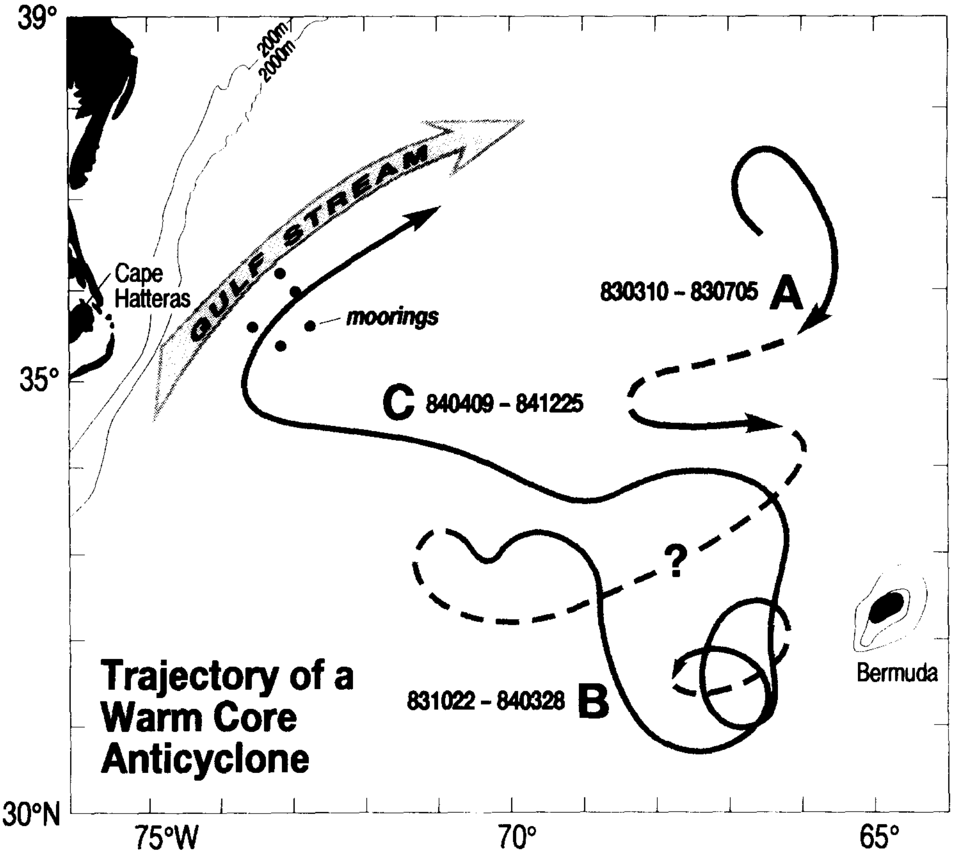

FIG.9(B) A schematic of the anticyclone's inferred trajectory. Solid line in B is when a float was continuously looping in the eddy; dashed line is the inferred path when no tracked float was in the eddy. Small dots show a current meter array that the eddy passed through (see BANE *et al*, 1989). Looper A (no.37) is from 83.03.10 - 83.07.05, 74 days plus a gap of 44 days when the float was not tracked but presumably kept looping. Looper B (no.44) is from 83.10.22 - 84.03.28 (158 days). Looper C (no.35) is from 84.04.09 - 84.12.25 (261 days). The short time gap of 11 days between loopers B and C, their similar looping characteristics, and the close proximity of loops, strongly suggest that loopers B and C are measurements of the same anticyclone over a 430 day period, a record for the western North Atlantic. The much larger gap of 108 days between loopers A and B casts doubt that these were in the same anticyclone despite their similar characteristics. If looper A was indeed an earlier measurement of the same anticyclone as loopers B and C, then this eddy was tracked for a total of 656 days.

anomaly of 4°C near this same depth, accompanying a dip in the thermocline of several hundred meters (Fig.10). The implied surface swirl velocity was around 20cm s^{-1}. The overall diameter was 150-200km, depending on the definition of the outer limit. The eddy first translated northeastward through the array at 14-17cm s^{-1}, then turned offshore and translated southwestward back through the array, around 50km from its earlier path. However, by this time the float had become entrained into the Gulf Stream and was being carried downstream; ending the continuous eddy tracking.

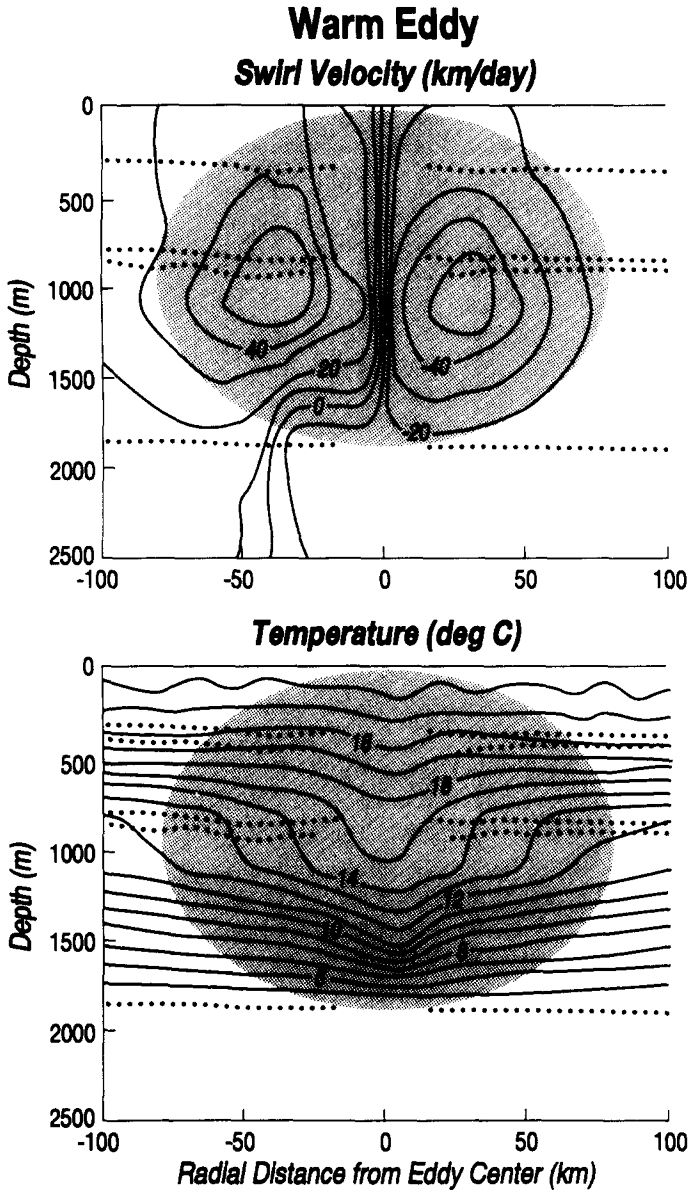

FIG.10. Characteristics of the warm anticyclone that translated through the current meter array (from BANE *et al*, 1989). The anticyclone's maximum swirl speed was greater than 50cm s^{-1} recorded at 900m at a radius of 30km. The maximum positive temperature anomaly was 4°C at 900m and coincided with a several hundred meter dip in the thermocline. (The implied thermostad between 15° and 16°C could be due to the way the temperatures were interpolated.) Velocity observations suggested a reduced velocity at the surface. The overall diameter was 150-200km depending on the definition of outer limit. The anticyclone first translated northeastward through the array at 14-17cm s^{-1}, turned offshore, and returned southwestward through the array ~50km farther offshore than its earlier path. By this time, the float had come out of the anticyclone and was advected downstream in the Gulf Stream. Interactions with the Gulf Stream by this and other anticyclones appear to be common in this region.

This anticyclone and others southeast of Cape Hatteras suggest that in this region interactions between anticyclones and the Gulf Stream are common (Fig.8B,C). Four other anticyclones translated westward into the Stream and then downstream (Fig.8C). The ultimate fate of these anticyclones is probably complete coalescence with the Gulf Stream, similar to that observed with cold-core rings. The opposite rotation direction in anticyclones could cause a different kind of interaction with the Gulf Stream and a different kind of final coalescence, however. Thus how an anticyclone finally dies remains speculative. Comparing float trajectories in this long-tracked anticyclone with those in cold-core rings suggests that this anticyclone was of similar size and had roughly the same period of rotation. Its swirl speed was around 35cm s^{-1}, versus 45cm s^{-1} for the fastest swirl speeds in cyclones (rings). However, the moored current meters measured an even faster swirl speed of 50cm s^{-1}, so the floats evidently missed the zone of highest velocity in the eddy.

Numerous warm-core eddies have been reported in the Sargasso Sea, in agreement with the warm cores of anticyclonic loopers. CORNILLON, EVANS and LARGE (1986) and SEAVER (1987) discussed eddies with warm surface cores that form from the Gulf Stream but are not rings. In a study of historical XBTs in the western Sargasso Sea, LAI and RICHARDSON (1977) found that around 2% of the data at 600m showed warm anomalies corresponding to a thick 18°C layer accompanied by a downward displacement of the thermocline of at least 150m. Ten possible warm core eddies were identified, six of which were south of but close to the Gulf Stream east of Cape Hatteras. These warm core eddies were inferred to be anticyclonic. Approximately one in four temperature anomalies was warm; the others being cold. EMERY, EBBESMEYER and DUGAN (1980) use swath XBT surveys (32°N-42°N, 20°W-60°W) to find 17 eddies, of which 5 (or 29%) were warm. The warm eddies had diameters of 100-200km. The ratio of warm to cold temperature anomalies corresponds reasonably closely to the ratio of anticyclonic to cyclonic looper data for the Gulf Stream region.

BRUNDAGE and DUGAN (1986) described a lens of 18°C water near 30°N 69°W that was 500m thick and 170km in diameter, with swirl speeds up to 50cm s^{-1}. They speculated that this anticyclone was a remnant of an eddy formed by a convection cell of 18°C water generated near the New England seamounts during the previous winter. They also give a good summary of earlier observations of warm lenses. The size of this eddy matches that of the loopers, so they could have been in similar eddies. Nineteen intrathermocline lenses were reported by DUGAN *et al* (1982) in the region 32-36°N 48-68°W. These tended to be smaller – less than 220m vertically and less than 65km in diameter – than most of the loopers. McWILLIAMS (1985) gives an excellent review of these eddies, which he calls submesoscale coherent vortices, and of various ways they could have formed.

9.1.2. Anticyclone formation. How warm-core anticyclones south of the Stream are formed is not known. The similarity of looping characteristics of no.46 (Fig.2C) and an anticyclone observed to form near the Corner Seamounts (36°N 52°W) suggests a similar mechanism for formation of some anticyclones. The evidence for the Corner Seamount eddy consists of several surface drifters and XBT surveys (RICHARDSON, 1980). These reveal that a branch of the Gulf Stream flowed southward at 30-135cm s^{-1} toward the Corner Seamounts. Two drifters originally in the Stream looped over and into the lee of the seamounts, suggesting that an anticyclone formed over the seamounts and then subsequently translated southwestward. The eddy's surface swirl speed was 30cm s^{-1} and its diameter was around 200km. The XBTs showed the thermocline to be depressed near the center of the eddy; the 15° isotherm reached 715m. A second anticyclone was also observed to drift southwestward in the lee of the Corner Rise. The implications from the three surface drifters are that warm-core anticyclones periodically form near the seamounts and subsequently drift southwestward at a rate of around 5cm s^{-1}. RICHARDSON (1980) discussed these observations in the light of models of anticyclones formed by flow past seamounts (HOGG, 1973; McCARTNEY, 1975, 1976; HUPPERT and BRYAN, 1976).

The clustering of several anticyclones in the northwestern part of the Sargasso Sea in close proximity to the Stream suggests that the Gulf Stream or the deep layer of 18°C water adjacent to it could have led to their formation. The 18°C water is a thick, nearly homogeneous layer centered in the northwestern Sargasso, where the main thermocline is particularly deep. XBT surveys have revealed spots where the main thermocline is even deeper, usually adjacent to the Stream and between cold-core rings. According to WORTHINGTON (1959) the deepest spots often occur in late winter, when the surface water south of the Stream has cooled to around 18°C and deep layers of vertically homogeneous water are formed. WORTHINGTON (1977) and LEETMAA (1977) observed a particularly deep layer in which the 18°C water extended down to 600m with the thermocline depressed beneath it, so that the 15°C isotherm, which normally lies near 650m, reached 845m. This deep depression of the thermocline was surrounded by an anticyclonic eddy (LEETMAA, 1977).

Anticyclones could form from parcels of 18°C water that separate from the thick layer adjacent to the Stream and then translate southward into a region of locally thinner 18°C water (as suggested by BRUNDAGE and DUGAN, 1986). Each eddy so formed would consist of a thick layer of 18°C water with the thermocline depressed beneath it, geostrophically corresponding to anticyclonic rotation above the thermocline. The formation of these 18°C water eddies and Mediterranean Water eddies is conceptually similar. In both cases, a mass of water consisting of a local minimum of potential vorticity separates from its source and is injected into a surrounding region of higher potential vorticity.

The energetic meandering of the nearby Gulf Stream could initiate 18°C water anticyclones by locally forming deep spots in the thermocline that may be further intensified by wintertime buoyancy forcing. If this hypothesis is correct, we might expect the most energetic anticyclones to form preferentially in late winter, next to the Stream. The inferred beginning of the longest tracked anticyclone (Fig.9) is south of the Gulf Stream in late winter (March 10, 1983), coincident with the deepest vertically mixed layers (Fig.11).

Evidence for the formation of anticyclones by the Gulf Stream is given by numerical models. These simulated anticyclones have been called opposite vortices (IKEDA and APEL, 1981), near-field eddies or near-field anticyclones (ROBINSON, SPALL and PINARDI, 1988), and near-field circulations (SPALL and ROBINSON, 1990). The formation of anticyclones modelled by SPALL and ROBINSON (1990) occurs immediately south of the Stream on the upstream side of a partially surrounding meander as a cyclonic ring pinches off (see their Figs 12, 16, 22). This simulated formation of anticyclones resembles the inferred formation of the observed anticyclone as shown in Fig.11.

PRATT, EARLES, CORNILLON and CAYULA (1991) have suggested that outbreaks of warm water (CORNILLON *et al*, 1986) from the Stream containing anticyclonic cores can be triggered through nonlinear steepening of long wave disturbances in the Stream. These warm water outbreaks involve both sinuous and varicose motions (varicose refers to variations in the Stream's width). Another possible trigger could be the short-range interaction of a cold core ring and the Stream; such interaction tends to be strongly nonlinear and can result in stripping of water from the edge of the Stream (BELL and PRATT, 1992). The detached water and ring can then propagate as a vortex pair away from the Stream. Until these models are expanded to include more vertical layers, the relevance of these latter two suggestions to the real Stream and anticyclones remains questionable.

The sources, sinks, births, deaths, and hydrographic properties of anticyclones remain poorly known. Firstly, they are less common and slightly less intense than the cyclonic rings which occur in the same area. Secondly, the swirl speed of the anticyclones seem to slow towards the surface whereas the swirl speed of rings is maximum there, making the latter easier to detect with near-surface measurements. Thirdly, sea surface temperature is a relatively poor indicator of anticyclones.

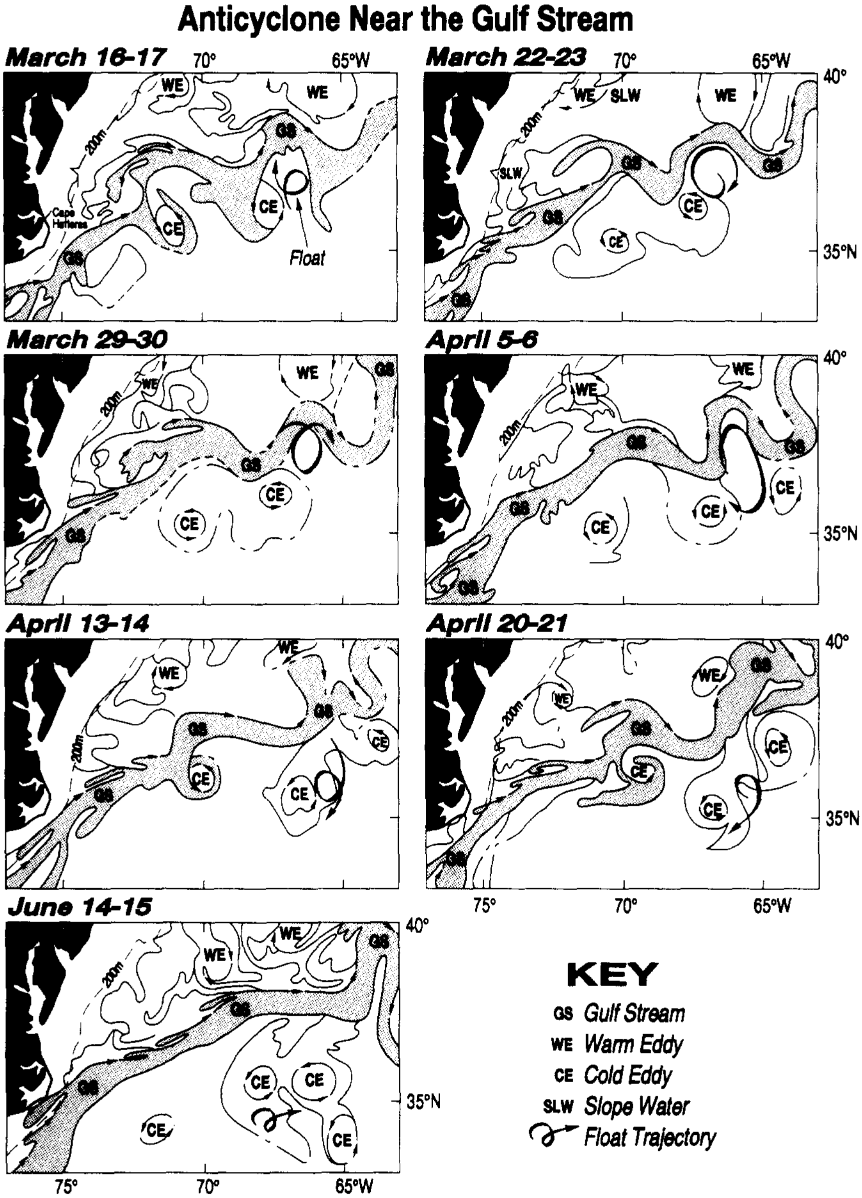

FIG. 11. Two-week pieces of looper no.37 in a warm core anticyclone (see Fig.9) superimposed on weekly schematic interpretations of satellite infrared images produced by the National Earth Satellite Service of the National Weather Service. The float began to loop anticyclonically near 37°N, 67°W just south of a northward projecting Gulf Stream meander and northeast of a cold core eddy or Gulf Stream ring that looked as if it was attached to the Gulf Stream (March 16, 1983). The anticyclone drifted eastward and then southward as a second cold core ring formed east of it (March 23 - April 13). On April 20 the anticyclone was a little southeastward of the midpoint between the two cold core rings and translated southwestward around the western ring. On June 15 the anticyclone translated eastward in the vicinity of three cold rings located to its north, northeast, and east. This last schematic is almost two months after the next-to-last one because of a gap in the float trajectory from April 23 - June 7.

It is ironic that much of the interest in mesoscale eddies was sparked by John Swallow's 1959 discovery of the energetic Aries eddy using subsurface floats (SWALLOW, 1961). The characteristics and location of the Aries eddy are similar to those of the anticyclonic eddies measured with more recent floats. Yet our knowledge of this species of eddies lags that of Gulf Stream rings, whose formation and demise have been witnessed repeatedly.

9.2 Western boundary region south of 30°N

In the southwestern North Atlantic (south of 30°N) the average swirl velocity of 700m loopers was 14 ± 1cm s^{-1} and their average diameter was 82 ± 12km, about half as fast and somewhat smaller than loopers nearer the Stream. Maximum values at 700m were around 20cm s^{-1} for both cyclones and anticyclones, and their average swirl velocity values calculated separately were similar, as were their temperatures.

The 700m loopers in the Sargasso Sea generally drifted westward toward the western boundary (as defined by the 2000m depth contour) where four of the cyclones went northward (north of 25°N) and one went southward (Fig.8). Eight of the ten 700m loopers south of 30°N and within 200km of the boundary (5 cyclones, 3 anticyclones) had a velocity component northward along the boundary, the other two (one cyclone, one anticyclone) had a southward component. The general trend of looper trajectories thus implies a northward boundary current in the upper layer.

In contrast to this, the trajectories of the deeper loopers imply a southward boundary current. Two 2000m floats drifted southeastward, generally within 100km of the boundary, with velocities of 10-15cm s^{-1} (see OWENS, 1991). The two loopers tracked by these floats also drifted southeastward, a cyclone at 4cm s^{-1} and an anticyclone at 15cm s^{-1}. One other 2000m cyclone observed 500km from the boundary drifted northwestward. One of the two 1300m loopers (both cyclones) in this region also drifted southward along the boundary from 30°-26°N; the other drifted southwestward toward the boundary. A few additional 1300m floats drifted southward within 100km of the boundary between 25°-30°N. Thus, the evidence from the mid and deep levels suggests that there is a narrow southward-flowing western boundary current that advects the eddies embedded in it.

The inferred mean northward translation of eddies at 700m and southward translation of eddies at 1300m-2000m is in agreement with the direction of western boundary currents at these depths. Historical shipdrift measurements clearly indicate mean northwestward surface velocities of 11 ± 1cm s^{-1} near the western boundary. LEE, JOHNS, SCHOTT and ZANTOPP (1990) found a northward flow near the Bahamas boundary (26.5°N) at depths of 300m-1000m and a southward flowing deep western boundary current below 800m with a core of 20cm s^{-1} near 2500m and 25km seaward of the western boundary. In order to investigate the boundary flow with float data, average velocities of floats within around 100km of the western boundary were calculated (Table 7). The 700m floats suggest a southward flow of around 2.0 ± 1.2cm s^{-1}, seemingly at odds with the northwestward trend of loopers. Since 700m floats lie near the boundary of northward and southward flow, the mean southward float velocity may be the upper part of the deep western boundary current, while most of the eddies at 700m are probably advected by the stronger northward flow 20cm s^{-1} just above this level and closer to the western boundary (see Figs 4a,5 by LEE *et al*). The two eddies that went south may have been advected by southward flow in the deep western boundary current. Evidence of the southward-flowing deep western boundary current from 1300m and 2000m floats is good (Fig.12). The mean velocity of all 1300m-2000m floats within around 100km of the 2000m contour was 7.4 ± 1.5cm s^{-1} southsoutheastward, where the 1.5cm s^{-1} standard error is an average of the east and north errors (Table 6). Additional evidence for the advection of eddies by the deep western boundary current was reported by LAI (1984), who analyzed current meter records east of the Blake Plateau.

TABLE 7. Southwestern Sargasso Sea (20-30°N, 65-77°W)

	Nobs	Ndf	$\overline{u}$ (cm s^{-1})	$\overline{v}$ (cm s^{-1})	EKE (cm^2 s^{-2})
A. Surface shipdrifts					
near western boundary	12301	–	-8.7 ± 1.3	6.8 ± 0.7	–
interior	64360	–	-4.2 ± 0.7	3.2 ± 0.3	–
B. 700m nonloopers					
near western boundary	506	80	-0.3 ± 1.2	-2.0 ± 1.2	58
interior	4868	652	-0.8 ± 0.4	-0.4 ± 0.4	43
C. 1300m - 2000m floats					
near western boundary	504	82	2.8 ± 1.3	-6.9 ± 1.6	90
interior	10660	1269	-0.8 ± 0.2	-0.4 ± 0.2	20

Average velocity values were calculated by grouping float and historical shipdrift data that fell within 1°x1° boxes lying along the western boundary (2000m depth contour). These averages are referred to above as "near western boundary". In addition all data that fell between 65°W and a line lying around 200km seaward of the boundary, and between 20°N and 30°N, were also grouped. These averages are referred to above as "interior". The 1300m and 2000m floats were merged to increase the numbers of observations and decrease standard errors.

Several of the individual eddies in this southwestern region have been discussed previously, by McDOWELL and ROSSBY (1978), RISER *et al*, (1978), ROSSBY, RISER and MARIANO (1983), ELLIOTT and SANFORD (1986), RISER *et al* (1986), and ROSSBY, PRICE and WEBB (1986). Anomalous water characteristics observed in eddies in the Polymode LDE and their inferred origin was discussed by McDOWELL (1986), LINDSTROM and TAFT (1986), and EBBESMEYER, TAFT, McWILLIAMS, SHEN, RISER, ROSSBY, BISCAYE and ÖSTLUND (1986). What is new here is the larger number of eddies identified by loopers and the conclusion that they are advected by western boundary currents.

9.3 Sargasso Sea

Since loopers near the Gulf Stream and the western boundary south of the Stream appear to be advected by currents in those regions, calculating mean translation rates for eddies there is problematic. In the Sargasso Sea clear of the Stream and western boundary 39 loopers have been observed, 23 cyclones and 16 anticyclones, a reasonably large sample for estimating the mean translation velocity. Their average velocities, obtained by grouping the individual translation velocities, were $\overline{u} = -2.8 \pm 0.4$cm s^{-1}, $\overline{v} = -0.4 \pm 0.4$cm s^{-1}, or 2.8cm s^{-1} toward 262° (Table 5). The meridional component is small and insignificantly different from zero, so these loopers appear to have been translating directly westward. The westward velocity of the cyclones was $\overline{u} = -3.0 \pm 0.4$cm s^{-1} and that of the anticyclones was very similar $\overline{u} = -2.5 \pm 0.7$cm s^{-1}. The 700m loopers translated slightly faster, $\overline{u} = -3.0 \pm 0.5$cm s^{-1}, than deeper ones, but as the number of deeper loopers was quite small this difference is insignificant. The average diameter of the 39 loopers was 88 ± 8km, so at 2.8cm s^{-1} an average eddy moving at 2.8cm s^{-1} took 36 days to pass a fixed point. This Eulerian period is somewhat longer than the Lagrangian average period of rotation of the 39 loopers, 22 ± 2 days.

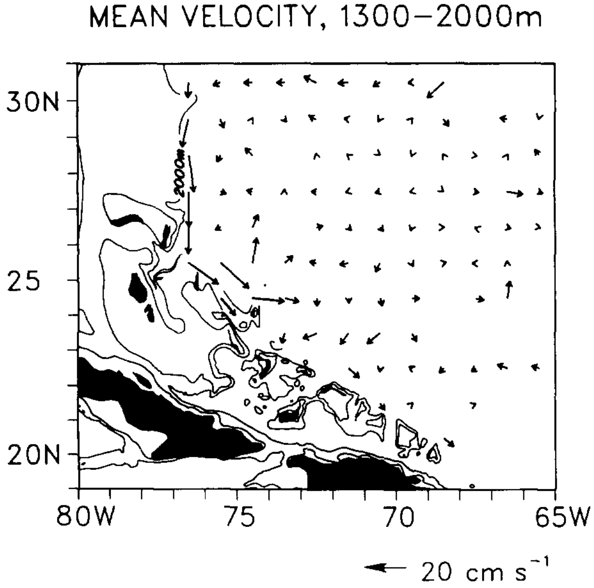

FIG.12. Mean velocity in the southwestern Sargasso Sea calculated by grouping all 1300m and 2000m floats into 1°x1° bins. Mean southward (north of 26°N) and southeastward (south of 26°N) velocities lie along the western boundary as defined by the 2000m depth contour. See Table 7 for a statistical summary.

An important issue is whether the loopers in the Sargasso Sea translated westward through background water of nearly zero velocity, or whether they were advected by the background flow field. The westward velocity of loopers is close to the beta-induced westward motion of eddies estimated from models, typically 1-2cm s^{-1} depending on the eddy parameters (CUSHMAN-ROISIN, CHASSIGNET and TANG, 1990; NOF, 1981; FLIERL, 1977). However, most of the Sargasso Sea loopers were found at 700m just south of the Gulf Stream where the Gulf Stream recirculation has been observed in float data (OWENS, 1991; RICHARDSON, 1985). Evidence from 700m floats in this recirculation region shows that the looper velocity $u = -2.3 \pm 1.8$cm s^{-1} is roughly equal to the nonlooper velocity $u = -1.6 \pm 0.6$cm s^{-1} (Table 4), which implies that the loopers could have been advected by the recirculation flow field. Qualitative evidence is added from both loopers and nonloopers that drifted westward in the recirculation into the Gulf Stream where they went downstream (OWENS, 1991). The nonlooper velocity in the recirculation region is significantly larger than the nearly zero velocity, $u = -0.1 \pm 0.3$cm s^{-1}, calculated from 700m nonloopers in a larger Sargasso Sea box, 25°-35°N, 50°-70°W. (Table 4). This difference appears to result from some floats, which drifted eastwards south of the recirculation (see OWENS, 1991), cancelling the mean westward velocity of floats in the recirculation. Virtually no looper data were available from this southern region (25°-30°N, 50°-70°W).

Swifter currents above 700m could also have exerted a force on the upper part of the eddies and thus helped advect them, as argued for Meddies by RICHARDSON *et al* (1989). Since the line of zero mean eastward velocity from historical shipdrifts lies near 32°N, which is near the center of the group of loopers in the recirculation, the evidence is for sluggish mean near-surface velocity near these loopers. A few loopers were located farther south, where the mean surface velocity from shipdrifts is westward at 4-5cm s^{-1}.

10. NEWFOUNDLAND BASIN

Nineteen loopers were found east of 47°W in the Newfoundland Basin, all at 700m except for one at 1150m (Fig.13). Fifteen of these loopers were traced by floats launched in this region, and the other four by three floats that drifted there in an extension of the Gulf Stream. Overall, loopers made up 47% of the 700m float data from the Newfoundland Basin experiment, and 41% of the total available 700m float data in the Newfoundland Basin. This implies that almost half of the area consists of eddies.

The loopers appear to be divided geographically into two groups. Nine loopers lay along the main front that corresponds to the northward current (Fig.13), and 10 were clustered near 40°N 40°W just east of the Newfoundland Ridge. Of the nine along the front, five were advected downstream and three of these split off and curved southward. Three others translated generally counter to the front, implying a recirculation of eddies close to the front. Some of the eddies in the cluster could have translated there from the front, but none was observed to do so. Several floats drifted southeastward from the frontal region toward the cluster, but they did not loop on their way toward the cluster, only when they arrived there.

The extent to which the Newfoundland Basin is filled with eddies is illustrated by float NB99, which looped for 560 days in seven different eddies and made numerous single loops. This float drifted very quickly from eddy to eddy, some cyclonic, some anticyclonic. The seven different eddies were difficult to distinguish because the loops are so convoluted and tightly grouped. The longest looper in the Newfoundland Basin was no.87, which looped for 277 days cyclonically in the vicinity of the eddy cluster (Fig.3). The characteristics of the 10 cluster loopers are rather similar. On average, they had a rotation period of 26 days, a swirl velocity of 18cm s^{-1}, a diameter of 116km, and a mean translation velocity of 1.4cm s^{-1} toward 215°. The average velocity from nonloopers in this region (Table 4) was eastward at 2.4cm s^{-1}, which may account for the low westward looper velocity. The mean eastward surface velocity in this region from historical shipdrifts is 7.4cm s^{-1}. Because of the complicated current structure, the small number of float observations does little to resolve the mean flow.

Three of the cluster of 10 loopers were anticyclones, accounting for 22% of the looper days. The anticyclones drifted somewhat faster (3.1cm s^{-1} toward 221°) than did the cyclones (0.6cm s^{-1} toward 203°), but the difference is probably not significant considering the few loopers and their convoluted trajectories.

The average percentage of looper days in a 10-degree-square bin encompassing the cluster, 33°-43°N, 35°-45°W, is 55%. If we interpret the 55% as representing the percentage of the area that consisted of eddies, we can speculate about what the eddy field might look like in the Newfoundland Basin. Using the average diameter of the 10 loopers, we infer that approximately 49 eddies could coexist in the box. Since 78% of the looper data are cyclonic, roughly 38 of the 49 would be cyclones and 11 anticyclones. If the packing of eddies were triangular, then the average separation between eddy centers would be 149km and between edges 33km (Fig.14)

Why does the Newfoundland Basin contain such a large percentage of eddies in general, and specifically of cyclones? A possible explanation involves the geometry of the western boundary and the way a branch of the Gulf Stream enters the basin. Figure 15A shows a schematic summary of the current system southeast of the Grand Banks as proposed by MANN (1967). The Gulf Stream flows eastward along the southern side of the southeast Newfoundland Ridge, where a branch separates near 39°N 43°W, turns and flows northwestward on the northern side of the Ridge, merges with the Slope Water Current to form the Atlantic Current. A southeastward projecting wedge of cold water overlies the Ridge. Occasionally parcels of this cold water pinch off to the

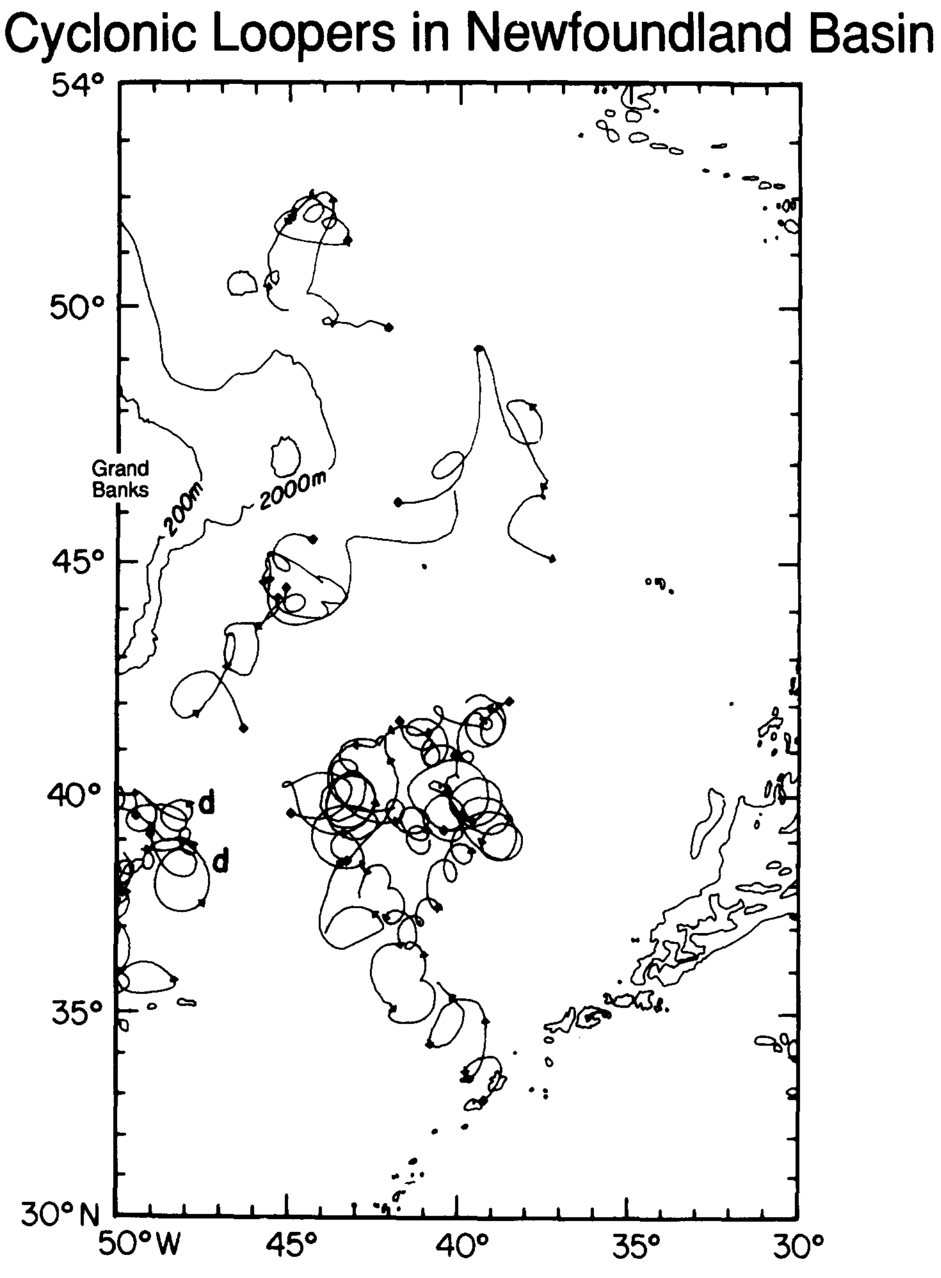

FIG.13. (A) Newfoundland Basin cyclonic loopers.

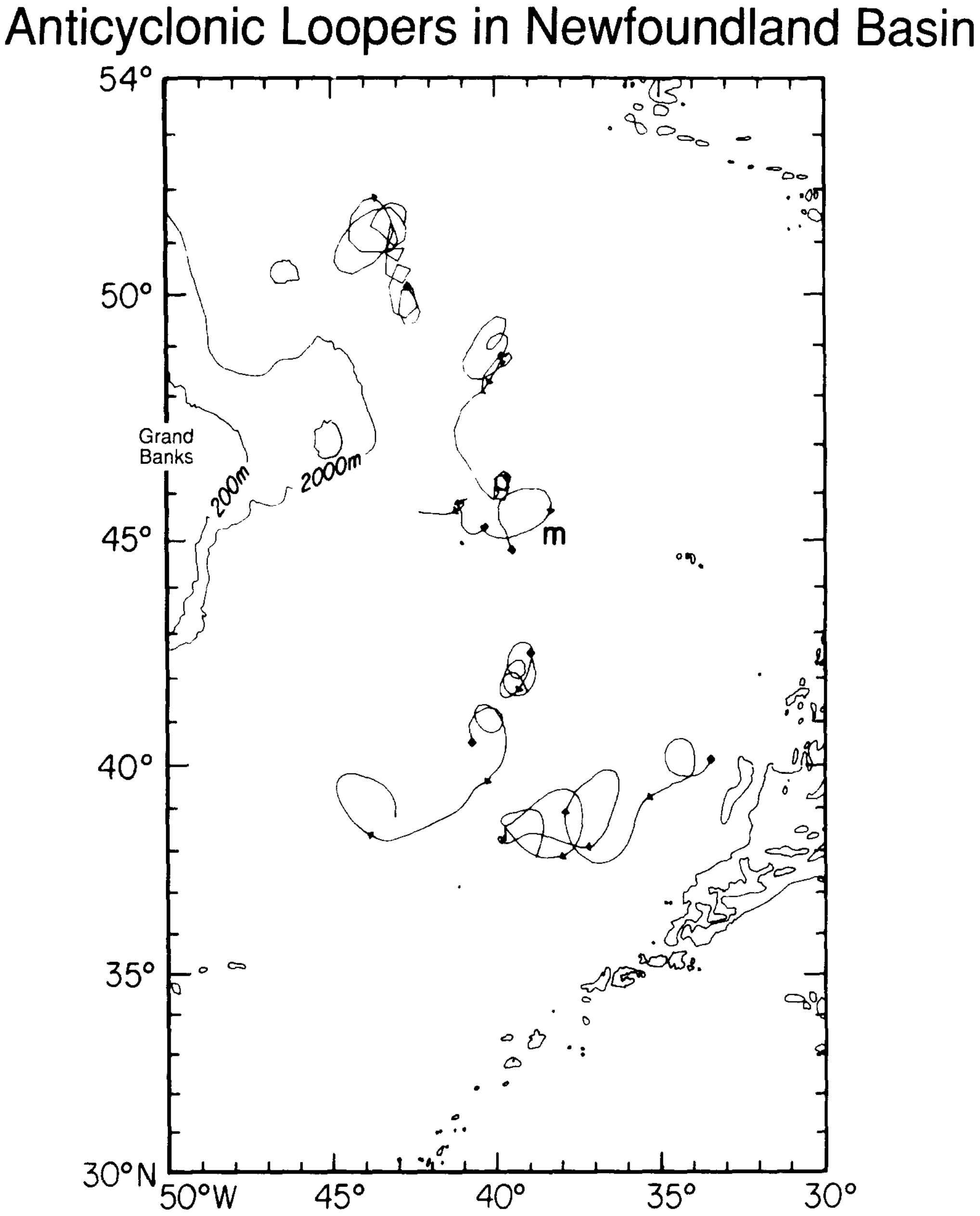

FIG.13(B) Newfoundland Basin anticyclonic loopers.

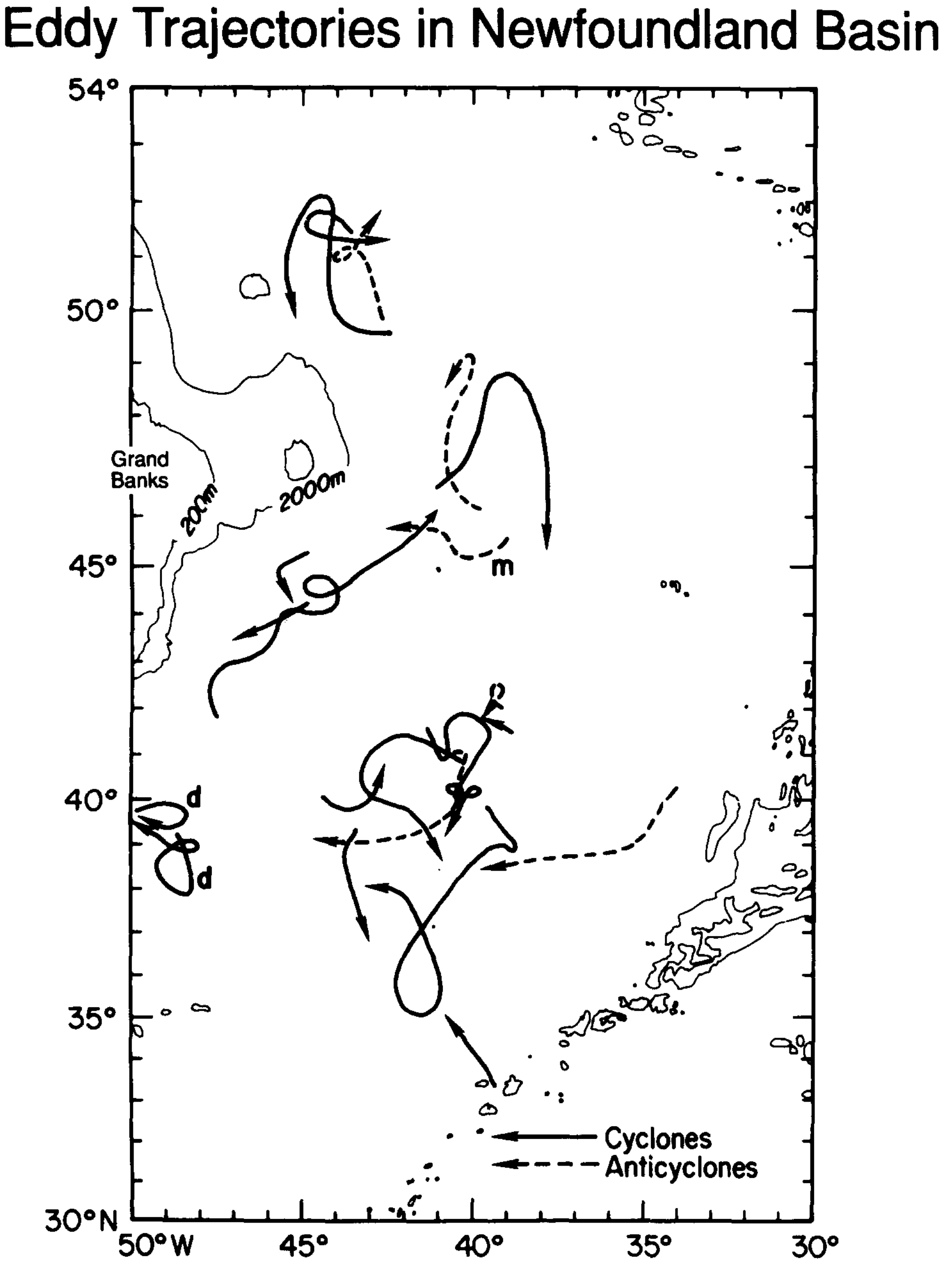

FIG.13(C) Trajectories of eddies inferred from loopers. Solid lines are cyclones, dashed anticyclones. Ten eddies in the interior of the basin near 40°N 40°W on average drifted southwestward at 1.2cm s^{-1}. Five eddies located in the Gulf Stream's extension in the basin seem to be advected downstream by this current. Three others nearby drifted counter to it.

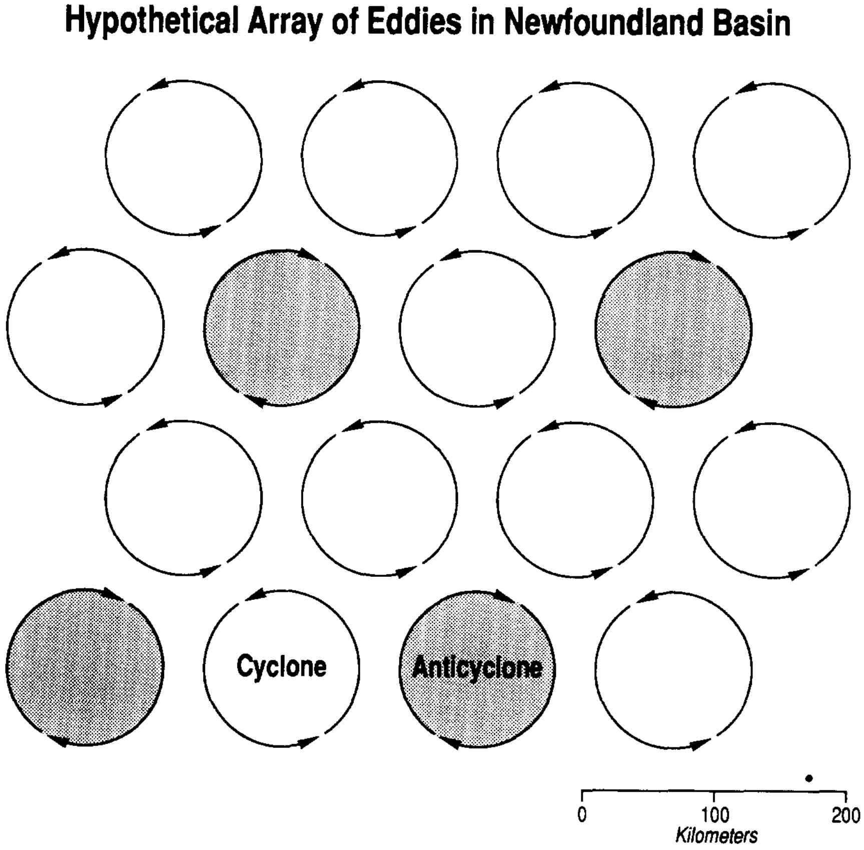

FIG.14. Hypothetical distribution of eddies in the Newfoundland Basin (33°N-43°N, 35°W-45°W). These distributions are based on the following asumptions: (1) that the 55% of looper data represents the percentage of the area consisting of eddies, (2) a mean looper diameter of 116km, and (3) a 1:3 ratio of anticyclones to cyclones.

southeast, forming cyclonic cold core rings (MANN, 1967; CLARKE, HILL, REINIGER and WARREN, 1980; MOUNTAIN and SHUHY, 1980; LaVIOLETTE, 1981). The left hand turn of the current around the Ridge might enhance eddy shedding at this point, and the turn might also initiate meanders in the current downstream of the Ridge that could grow and eventually form eddies. Most of the loopers, 70-78% depending on whether one counts individual loopers or looper days, are cyclonic, similar to eddies that pinch off from the cold water over the Ridge.

Characteristic paths of water are shown by six floats, all at 700m, that drifted from the west around the Newfoundland Ridge into the Basin (Fig.15B). Four of the six turned sharply left (cyclonically) in the vicinity of the Ridge before entering the Basin where they meandered and looped. One float (SL143) drifted eastward into the eddy cluster near 40°N 40°W and looped cyclonically there for 143 days (no.84). This float may have been trapped in an eddy just as it pinched off from a meander east of the Ridge and thus may show how the cyclonic eddies in the cluster originate.

The origin of the anticyclones in the Newfoundland Basin is unknown, but their similarity to those near the Gulf Stream and the similar percentage of anticyclonic looper data (~1/4) in both

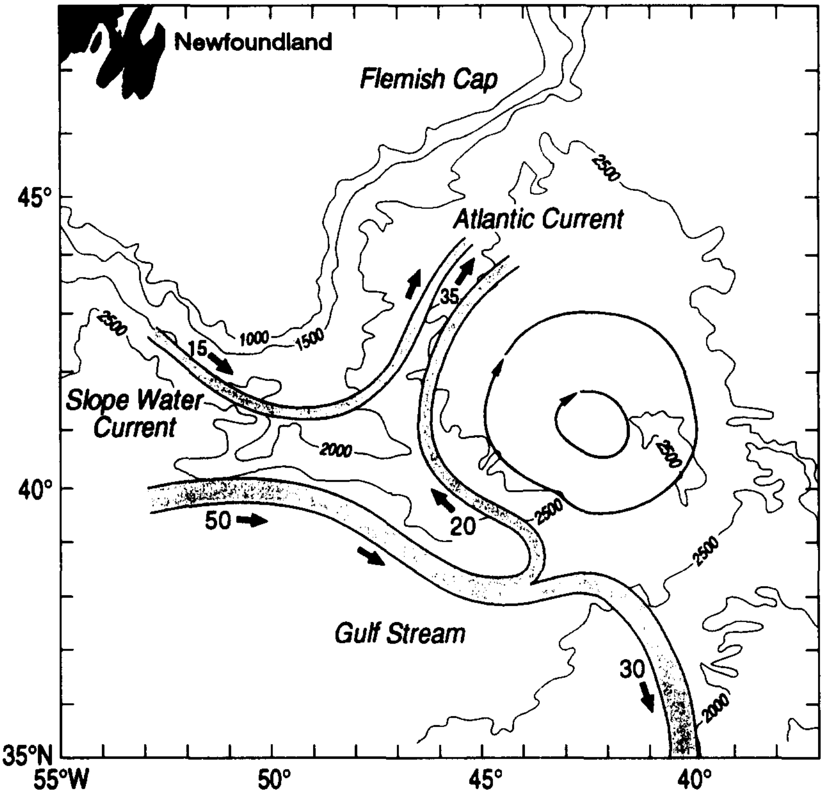

FIG.15. (A) A schematic summary of the current system southeast of the Grand Banks as proposed by MANN (1967). Volume transport in units of $10^6 m^3 s^{-1}$ is given for each current. Large temporal fluctuations occur in the pattern of currents, so the schematic is much simplified. Details of the branching of the Gulf Stream have been described by CLARKE *et al* (1980).

regions suggests a common origin. In late winter, 600-1000m deep layers of isothermal water are formed in the Newfoundland Basin, like those south of the Gulf Stream discussed earlier (WORTHINGTON, 1976; MANN, 1967). The isothermal layers in the Newfoundland Basin tend to be cooler than those south of the Stream, below 15°C and sometimes even 14°C. Underneath the isothermal layers the thermocline is depressed; the depression of isotherms often extends below 2000m. Thus the anticyclones could be made up of this water. A good example of a large anticyclone near 41°N 42°W was described by MANN (1967). Its center consisted of isothermal water of 14.8°C overlying a depressed thermocline in which the 10°C isotherm was at 1150m, a greater depth than it normally attains in the Sargasso Sea. High oxygen values in the central water indicated that this anticyclone had formed the previous winter.

The swirl velocity of loopers in the Newfoundland Basin was generally less than near the Gulf Stream farther west. The average swirl velocity of 10 loopers near 700m in the cluster near 40°N 40°W was 18 ± 2cm s^{-1}. The three anticyclones in this cluster were slightly swifter, at 20 ± 1cm s^{-1}, than the seven cyclones, at 17 ± 2. The average diameter for both groups was similar to the average of all 10 loopers, 116 ± 12km. Two fast anticyclones were found farther north in this region; one at 40cm s^{-1} near 50°N 43°W (no.96) and the other at 32cm s^{-1} near 46°N 40°W (no.94).

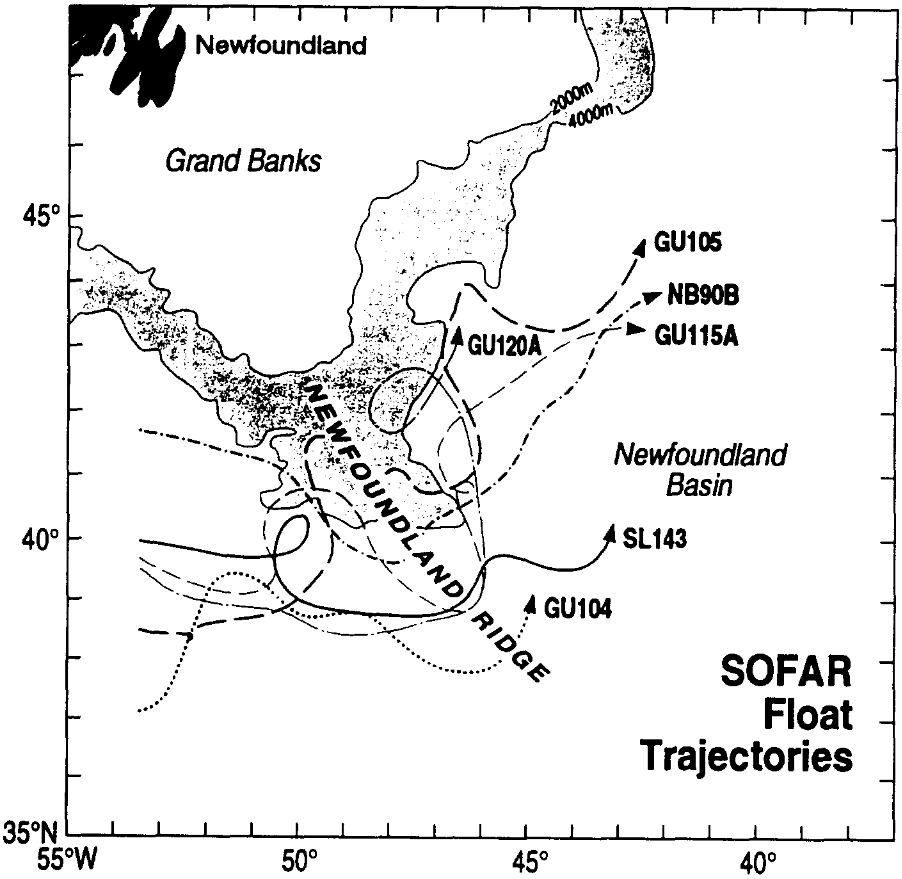

FIG.15.(B) Trajectories of six floats at 700m that entered the Newfoundland Basin from the west. For clarity, trajectories were terminated when they began to loop or became complicated. Float GU104 died near 39°N 45°W, SL143 looped near 40°N 43°W, and the other four continued to drift (on average) northeastward. The floats indicate an inflow from the Gulf Stream into the Newfoundland Basin, but the pattern appears to be more complicated than the schematic suggested by MANN (1967) based on hydrography. SCHMITZ (1985) discussed some of these floats that entered the Newfoundland Basin, and OWENS and ZEMANOVIC (1990) showed some individual trajectories there.

The 700m temperature of Newfoundland Basin cyclones in the cluster near 40°N 40°W was 7.8°C, 3.1°C colder than that of anticyclones (10.9°C). Anticyclonic loopers with smaller diameters (<100km) were colder (7.3°C) than larger ones (8.3°C). Cyclones were 1.8°C colder than nonloopers and anticyclones 1.3°C warmer.

11. EASTERN BASIN

Thirty-three floats were launched in the Eastern Basin, 32 near a depth of 1100m in the Mediterranean Water, and one near 200m as a test of a Bobber float by Jim Price. Seven of the 1100m floats were deliberately launched in two Meddies, anomalously warm and salty (~1°/oo) eddies approximately 100km in diameter and 0.8km thick. An additional float was launched in a third Meddy by chance. These Meddies (nos 103-110) are described by ARMI *et al* (1989) and RICHARDSON *et al* (1989). Briefly, Meddy 1 was followed for over 2 years during 1984-1986 as it drifted 1090km southward with a mean velocity of 1.8cm s^{-1} (Figs 16,17). Four shipboard surveys revealed the nearly total decay of Meddy 1 by gradual mixing processes. Meddy 2 drifted 530km southwestward over 8.5 months with a mean velocity of 2.3cm s^{-1} until it collided with Hyères Seamount and the two floats in it stopped looping abruptly, implying a major disruption if not total destruction of the eddy. Meddy 3 drifted 500km southwestward for 1.5 years at 1.1cm s^{-1}.

New float data from 1986-1988 revealed an even longer life for Meddy 1 – 821 days and 114 loops, setting a record for continuous long-term eddy tracking (no.103). Two additional short loopers (nos 117,118) that translated northward in the lee (west) of the seamounts could be small pieces of the original Meddy 2 that crashed into the seamounts (Fig.16). The swirl speeds in these leeward eddies were 1/2 to 1/3 as fast and the period of rotation 3 to 5 times longer than that for Meddy 2.

Excluding the three Meddies, 11 other loopers were identified in the 1100m floats (Fig.16). All but three of these were anticyclonic, and the three cyclones were all short records (<63 days). Clearly, anticyclones dominate the 1100m layer. Four of the longest loopers (nos 111-114) give a new picture of three different anticyclones with similar characteristics. Two floats (nos 112,113) looped simultaneously in one anticyclone, and one float looped in two of the anticyclones (nos 113,114). This same float looped in the longest tracked of these anticyclones (no.114), which was followed for 318 days as it translated 630km westward up to but not across the mid-Atlantic Ridge. The average characteristics of the three anticyclones were a rotation period of 31 ± 3 days, a swirl velocity of 6.3 ± 1.0cm s^{-1}, a mean diameter of 48 ± 14km (with largest loops of 100km), and an advection velocity of 2.7cm s^{-1} toward 253° (Table 5). These anticyclones were roughly the same size as Meddies and rotated in the same direction but more slowly, with a slower swirl speed and had a weaker warm temperature anomaly.

After it stopped looping in one of these anticyclones (no.112), float EB133 experienced a drop in temperature and float EB137 experienced a rise in temperature (no.71) which suggests that the anticyclones have a positive temperature anomaly of at least 1.0°C. The corresponding positive salinity anomaly, calculated using the local T-S relation, is around 0.22 and the core anomalies could be larger still. However, these anticyclones do not meet the Meddy criterion of a positive salt anomaly of at least 0.4, used by RICHARDSON, McCARTNEY and MAILLARD (1991) to identify Meddies in historical data (see Fig.17).

The translation velocity of the anticyclones is more westward than the Meddy average but similar to that of Meddy 2, which was tracked nearby. Of all the 1100m Eastern Basin floats, the two that drifted the farthest west (EB133, EB137) were both trapped for various lengths of time in these anticyclones. By comparison, floats outside of eddies remained fairly close to their launch location.

Their similarity to Meddies suggests that these anticyclones are weaker brethren that also originate in the Mediterranean Water but farther west than the probable source of Meddies, which is thought to be the very salty Mediterranean overflow water near Cape St Vincent, Portugal. The Mediterranean tongue is less smooth than some small-scale maps of it imply (Fig.17). Closely

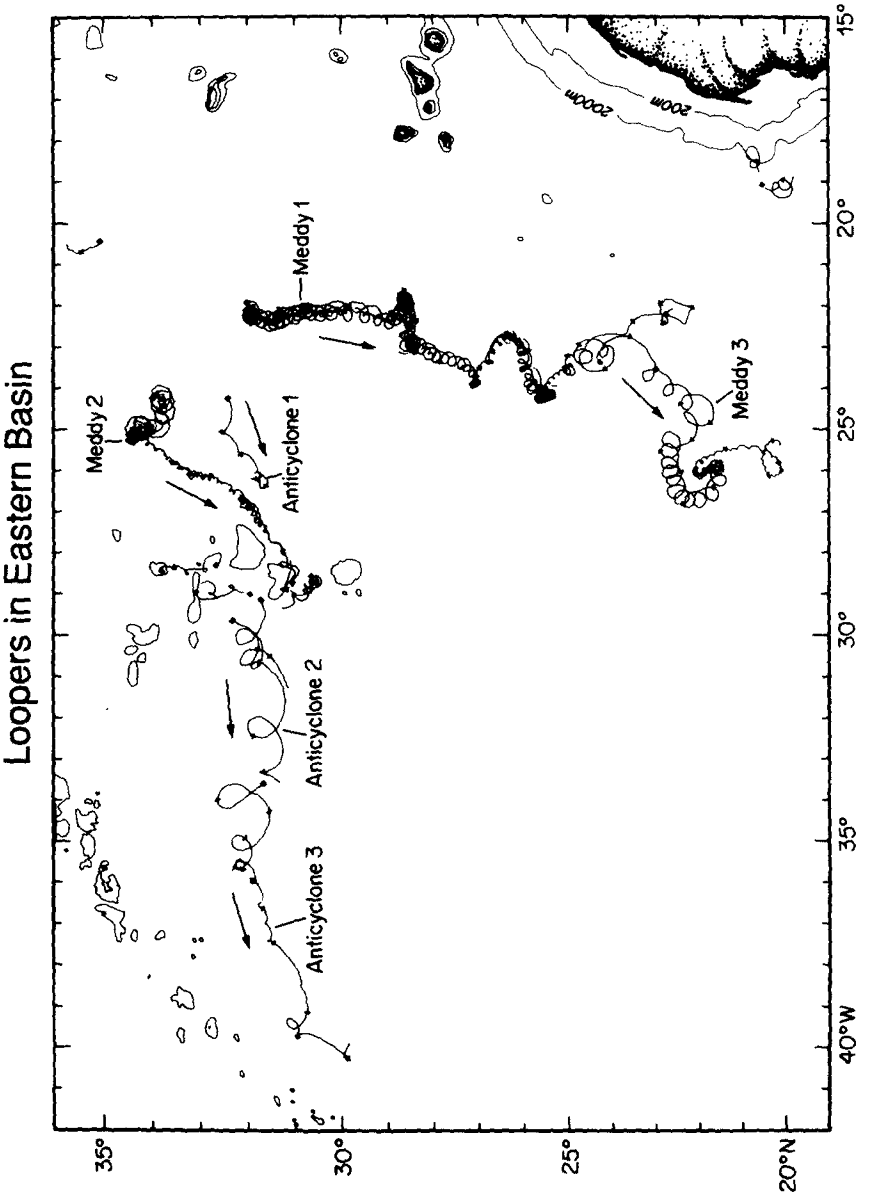

FIG.16. (A) Eastern Basin loopers, most of which were anticyclones.

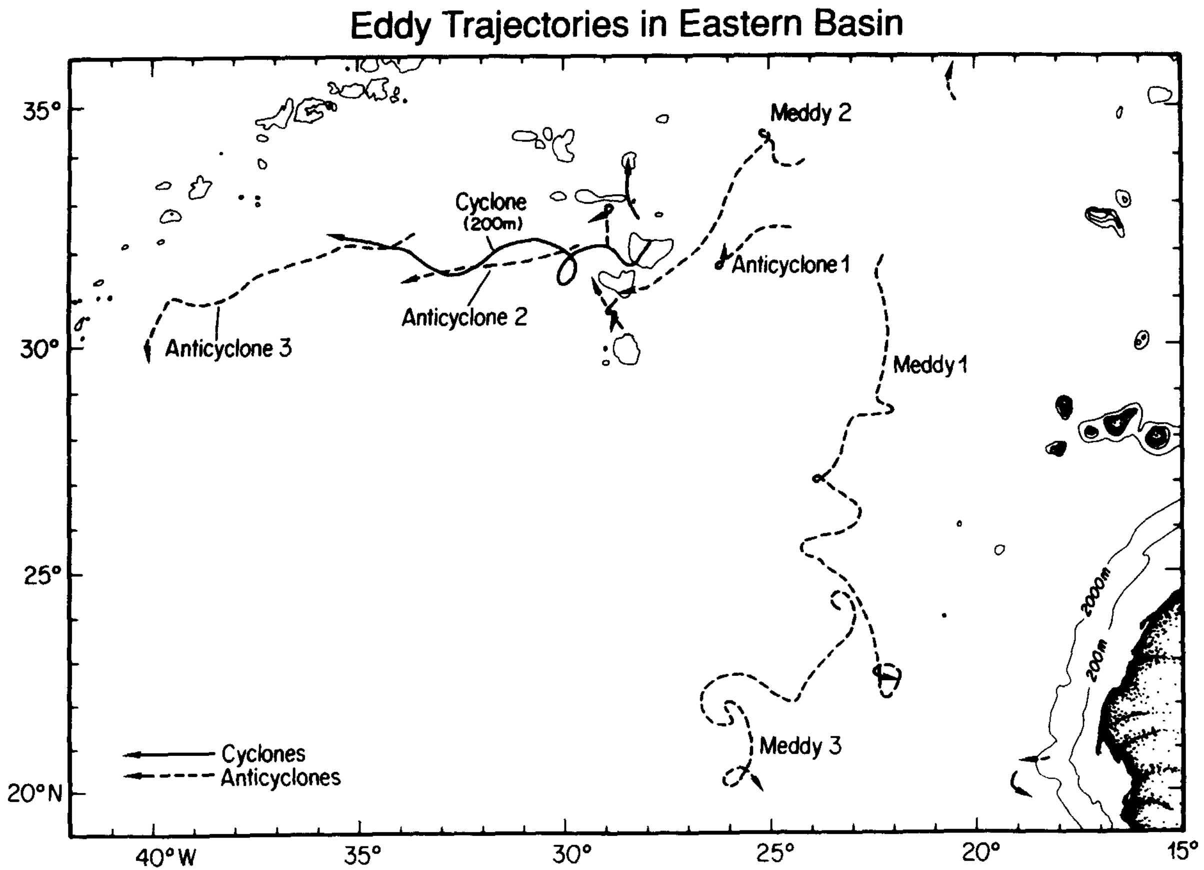
Eddy Trajectories in Eastern Basin

FIG.16.(B) Trajectories of eddies, inferred from the loopers. Three Meddies and three other anticyclones, similar but rotating somewhat slower than the Meddies, drifted on average southwestward at 1.5cm s^{-1}. Two Meddies drifted mostly southward; the three anticyclones drifted mostly westward. An extrapolation of the three anticyclones' track across the Atlantic intersects the western boundary close to the McDOWELL and ROSSBY (1978) salty lens. If no.114 had continued at its average velocity of 2.3cm s^{-1}, it would have reached the western boundary in an additional 4.2 years.

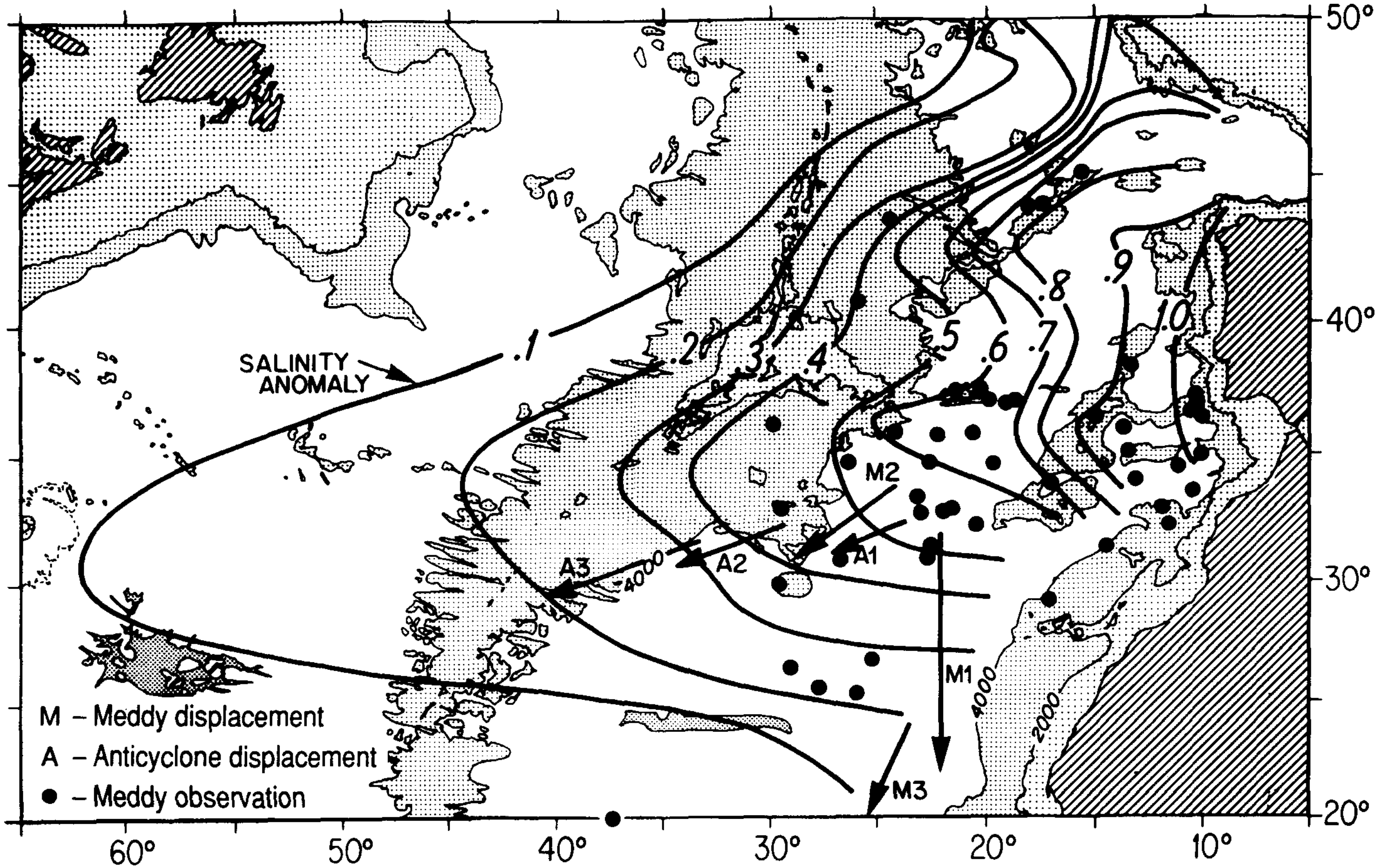

FIG. 17. Mediterranean water tongue and summary of Meddy observations (dots) and displacement vectors of three Meddies as shown by RICHARDSON *et al* (1991). Displacement vectors of the three additional anticyclonic eddies tracked continuously with SOFAR floats have been added (nos. 111, 112, 114). The three new anticyclones are similar to Meddies but rotate more slowly and contain weaker temperature anomalies. Contours of the salinity anomaly relative to 35.01psu near 1100db is based on a figure by NEEDLER and HEATH (1975) and shown by JOYCE (1981).

spaced stations reveal large variations of salt over small spatial scales (RICHARDSON *et al*, 1991). Blobs of anomalously salty water in the tongue, not salty enough to be Meddies, could pinch off from the tongue and drift westward into cooler, fresher water as anticyclones. KÄSE and ZENK (1987) suggested that Meddies could form in the vicinity of the Azores front as a result of meanders in this current which pinch off to the south as near-surface cyclonic eddies and that also transport deeper salty Mediterranean Water from farther north in deeper anticyclonic eddies. The very high salinity in Meddies seems to require that they originate near Cape St Vincent, but perhaps the less salty eddies observed here form this way.

The early history of the four floats in the anticyclones gives some clues to their possible formation. These four floats were launched with 10 others in a cluster near 32°N 24°W. During the first few months the cluster drifted coherently westward at a rate of a few cm s^{-1}. At this time float EB131, located on the northern side of the cluster, began to loop in the first anticyclone, near 32°N 25°W (no.111). After five months most floats returned eastward toward 31°N 24°W, where they gradually dispersed. Four floats, including EB133 and EB137, continued drifting westward along 32.5°N through a chain of seamounts near 28°W. West of the seamounts, EB133 and EB137 began to loop in the two other anticyclones. The temperature measured by these two floats was nearly constant from their launch until after they finished their first set of loops, implying that the anticyclone (nos 112,113) was composed of the same water in which the floats were launched.

A meridional hydrographic section through the float cluster at its launch site revealed two salinity maxima near 1100m. One of the 35.65 psu was in the float cluster at 32°N and may be related to the high salinity in the first anticyclone. The salinity anomaly was 0.17 psu compared to stations located north and south of the cluster. A second, larger maximum of 35.92psu was located further north at 37°N, but a float launched in the second maximum drifted generally northeastward. Thus the major westward flow in the vicinity of the salt tongue appeared to be near 32°N, coinciding with the float cluster and first anticyclone.

An interpretation of the data is that the floats were launched into a jet that was carrying warm salty Mediterranean Water westward. One of these floats looped in the first anticyclone for four months as it translated westward. Ten months and 500km later, part of the warm salty jet water passed through the seamounts into cooler fresher water there and split into two eddies which propagated westward. If this scenario is correct, then the floats revealed the formation site of these eddies. Another interpretation is that the floats had been carried westward in the jet and were entrained into already existing eddies which had propagated there from farther east. The nearly constant temperatures experienced by the two floats up until the time they left the anticyclone favors the first interpretation, as does the inferrence that eddies drifting through the seamounts are likely to break apart.

West of the seamounts from 30°W to 40°W, 19% of the float data are in the two western anticyclones. This implies that a significant portion of this region consists of anticyclones. However, the data may be biased by the way the floats entered this region in a salty jet. Considering all Eastern Basin floats at 1100m but excluding those launched deliberately in Meddies, we find more looper days in the three anticyclones (624 days) than in the one Meddy sampled by chance (549 days). This crude measure suggests that the anticyclones occur at least as often as do Meddies and that the anticyclones may be frequent west of the 28°W seamounts, where few trajectories were obtained. The implication is that these anticyclones could be important to the westward flux of salt and heat in the Mediterranean Water. To evaluate this importance, further work documenting their number and hydrographic properties is required.

The bobber float (EB014) was tracked in the Eastern Basin for a total of 599 days. For 261 days this float looped 10 times cyclonically at a mean depth of 220m as it translated westward along 32°N (from 28°W to 35°W) with a mean velocity of 4.4cm s^{-1} (no.99). This one shallow float shows that a different kind of eddy occurs near the surface, probably one formed from the Azores current to the north. GOULD (1985) observed the formation from the Azores front of a cyclonic cold core eddy 100-150km in diameter that subsequently drifted westward along 32°N (from 31°W to 37°W) at 2.5cm s^{-1}. The cyclone observed with the Bobber (and also Gould's eddy) translated westward directly over the paths of the two anticyclones at 1100m discussed above, but at a different time.

12. SUMMARY

U.S. SOFAR float data from the North Atlantic have been analyzed to obtain a new description of ocean eddies. The analysis used the Lagrangian nature of floats that became trapped in eddies and looped around their centers as they drifted through the ocean. The frequency of occurrence of several different kinds of eddies was determined, as well as their sizes, trajectories, swirl velocities, and translation velocities. These characteristics, estimated from looping trajectories, were used to compare eddies in different regions and at different depths. Limitations of the study are the inhomogeneous distribution of float trajectories and the lack of supporting measurements of water properties in the eddies. In addition, each looping float trajectory usually provided data at only one depth and one diameter, making comparison of eddies difficult and somewhat subjective.

One surprising result was the large number of energetic anticyclones observed at 700m in the Sargasso Sea, including one tracked for 430 days whose properties were well measured. These anticyclones rival cyclonic Gulf Stream rings in their numbers, sizes, and swirl speeds. It is speculated that they form near the Stream from deep layers of 18°C water.

A second surprising result was the particularly large number of eddies observed at 700m in the Newfoundland Basin, where approximately half of the area consisted of eddies, the highest percentage coverage observed. This large number of eddies could be caused by the way a branch of the Gulf Stream flows cyclonically around the Newfoundland Ridge into the Basin.

In the eastern Atlantic, three Meddy-like anticyclones were observed. These are weaker than Meddies but probably occur more frequently than Meddies, based on the percentage of loopers in them. Two anticyclones are thought to have originated when a westward jet of Mediterranean Water broke apart after passing through a line of seamounts near 29°W.

Eddies generally translated westward at a few cm s^{-1} except when they were advected by currents along the western boundary and in and near the Gulf Stream, where eddy trajectories became complicated. The mean westward translation rate of 39 eddies in the Sargasso Sea was 2.8cm s^{-1}. Many of these eddies were located just south of the Gulf Stream in its recirculation where they were probably avected by a westward current. The eddy kinetic energy of loopers was generally much greater than that of background floats. This suggests that the eddies are important dynamically and in causing the distribution of mean EKE in the ocean.

13. ACKNOWLEDGEMENTS

This is contribution 7933 from the Woods Hole Oceanographic Institution. Funds were provided by the National Science Foundation Grants OCE90-09463 and OCE89-16082. W.B. Owens, J.F. Price, H.T. Rossby, and W.J. Schmitz, Jr., helped obtain the float data and made them available for the looper analysis. H. Stommel showed me his vortex sea model float simulations which were helpful in spotting loopers. C. Wooding and M. Zemanovic helped identify loopers, calculate statistics, and plot results. M.A. Lucas typed the manuscript. D. Walsh suggested new ways to calculate statistics from loopers. J. Price, M. Spall, S. Schwartz and an anonymous reviewer made helpful suggestions on an earlier version of this paper.

14. REFERENCES

ARMI, L., D. HEBERT, N. OAKEY, J.F. PRICE, P.L. RICHARDSON, H.T. ROSSBY and B. RUDDICK (1989) Two years in the life of a Mediterranean salt lens. *Journal of Physical Oceanography*, **19**, 354-370.

BANE, J.M., L.M. O'KEEFE and D.R. WATTS (1989) Mesoscale eddies and submesoscale, coherent vortices: Their existence near and interactions with the Gulf Stream. In: *Mesoscale/Synoptic Coherent Structures in Geophysical Turbulence*, Proceedings of the 20th International Liege Colloquium on Ocean Hydrodynamics, J.C.J. NIHOUL and B.M. JAMART, editors, Elsevier, New York, 501-518.

BELL, G.I. and L.J. PRATT (1992) The interaction of an eddy with an unstable jet. *Journal of Physical Oceanography*, **22**, 1229-1244.

BRUNDAGE, W.L. and J.P. DUGAN (1986) Observations of an anticyclonic eddy of 18°C water in the Sargasso Sea. *Journal of Physical Oceanography*, **16**, 717-727.

CHENEY, R.E., W.H. GEMMILL, M.K. SHANK, P.L. RICHARDSON and D. WEBB (1976) Tracking a Gulf Stream ring with SOFAR floats. *Journal of Physical Oceanography*, **6**, 741-749.

CLARKE, R.A., H.W. HILL, R.F. REINIGER and B.A. WARREN (1980) Current system south and east of the Grand Banks of Newfoundland. *Journal of Physical Oceanography*, **10**, 25-65.

CORNILLON, P., D. EVANS and W. LARGE (1986) Warm outbreaks of the Gulf Stream into the Sargasso Sea. *Journal of Geophysical Research*, **91**, 6583-6596.

CUSHMAN-ROISIN, B., E.P. CHASSIGNET and B. TANG (1990) Westward motion of mesoscale eddies. *Journal of Physical Oceanography*, **20**, 758-768.

DOW, D.L., H.T. ROSSBY and S.R. SIGNORINI (1977) SOFAR floats in MODE. University of Rhode Island, G.S.O. Technical Report **77-3**, 108pp.

DUGAN, J.P., R.P. MIED, P.C. MIGUEREY and A.F. SCHUETZ (1982) Compact, intrathermocline eddies in the Sargasso Sea. *Journal of Geophysical Research*, **87**, 385-393.

EBBESMEYER, C.C., B.A. TAFT, J.C. McWILLIAMS, C.Y. SHEN, S.C. RISER, H.T. ROSSBY, P.E. BISCAYE and H.G. ÖSTLUND (1986) Detection, structure, and origin of extreme anomalies in a western Atlantic oceanographic section. *Journal of Physical Oceanography*, **16**, 591-612.

ELLIOTT, B.A. and T.B. SANFORD (1986) The subthermocline lens D1. Part I: Description of water properties and velocity profiles. *Journal of Physical Oceanography*, **16**, 532-548.

EMERY, W.J., C.C. EBBESMEYER and J.P. DUGAN (1980) The fraction of vertical isotherm deflections associated with eddies: An estimate from multiship XBT surveys. *Journal of Physical Oceanography*, **10**, 885-899.

FLIERL, G.R. (1977) The application of linear quasigeostrophic dynamics to Gulf Stream rings. *Journal of Physical Oceanography*, **7**, 365-379.

FREELAND, H.J., P.B. RHINES and H.T. ROSSBY (1975) Statistical observations of the trajectories of neutrally buoyant floats in the North Atlantic. *Journal of Marine Research*, **33**, 373-404.

GOULD, W.J. (1985) Physical oceanography of the Azores front. *Progress in Oceanography*, **14**, 167-190.

HOGG, N.G. (1973) On the stratified Taylor column. *Journal of Fluid Mechanics*, **58**, 517-537.

HUPPERT, H.E. and K. BRYAN (1976) Topographically generated eddies. *Deep-Sea Research*, **23**, 655-679.

IKEDA, M. and J. APEL (1981) Mesoscale eddies detached from spatially growing meanders in an eastward-flowing oceanic jet using a two-layer quasi-geostrophic model. *Journal of Physical Oceanography*, **11**, 1638-1661.

JOYCE, T.M. (1981) Influence of the mid-Atlantic Ridge upon the circulation and the properties of the Mediterranean Water southwest of the Azores. *Journal of Marine Research*, **39**, 31-52.

KÄSE, R.H. and W. ZENK (1987) Reconstructed Mediterranean salt lens trajectories. *Journal of Physical Oceanography*, **17**, 158-163.

KENNELLY, M.A. and T.K. McKEE (1984) Gulf Stream Recirculation Experiment (GUSREX) and Line Experiment SOFAR float data 1980-1982. *Woods Hole Oceanographic Institution Technical Report*, **WHOI-84-45**, 444pp.

LAI, D.Y. (1984) Mean flow and variabilities in the deep western boundary current. *Journal of Physical Oceanography*, **14**, 1488-1498.

LAI, D.Y. and P.L. RICHARDSON (1977) Distribution and movement of Gulf Stream rings. *Journal of Physical Oceanography*, **7**, 670-683.

LaVIOLETTE, P.E. (1981) Variations in the frontal structure of the southern Grand Banks. *Technical Note*, **87**, April 1981, NORDA, NSTL Station, Mississippi, 48pp.

LEE, T.N., W. JOHNS, F. SCHOTT and R. ZANTOPP (1990) Western Boundary Current structure and variability east of Abaco, Bahamas, at 26.5°N. *Journal of Physical Oceanography*, **20**, 446-466.

LEETMAA, A. (1977) Effects of the winter of 1976-77 on the northwestern Sargasso Sea. *Science*, **198**, 188-189.

LINDSTROM, E.J. and B.A. TAFT (1986) Small water-property transporting eddies: Statistical outliers in the hydrographic data of the POLYMODE Local Dynamics Experiment. *Journal of Physical Oceanography*, **16**, 613-631.

MANN, C.R. (1967) The termination of the Gulf Stream and the beginning of the North Atlantic Current. *Deep-Sea Research*, **14**, 337-359.

McCARTNEY, M.S. (1975) Inertial Taylor columns on a beta-plane. *Journal of Fluid Mechanics*, **68**, Part 1, 71-95.

McCARTNEY, M.S. (1976) The interaction of zonal currents with topography with applications to the Southern Ocean. *Deep-Sea Research*, **23**, 413-427.

McDOWELL, S.E. (1986) On the origin of eddies discovered during the POLYMODE Local Dynamics Experiment. *Journal of Physical Oceanography*, **16**, 632-652.

McDOWELL, S.E. and H.T. ROSSBY (1978) Mediterranean water: An intense mesoscale eddy off the Bahamas. *Science*, **202**, 1085-1087.

McKEE, T.K. (1986) A summaryof historical SOFAR float data in the western North Atlantic, 1972-1981. *Woods Hole Oceanographic Institution Technical Report*, **WHOI-86-24**, 722pp.

McWILLIAMS, J.C. (1985) Submesoscale, coherent vortices in the ocean. *Reviews of Geophysics*, **23**, 165-182.

MOUNTAIN, D.G. and J-L SHUHY (1980) Circulation near the Newfoundland Ridge. *Journal of Marine Research*, **38**, 205-213.

NEEDLER, G.T. and R.A. HEATH (1975) Diffusion coefficients calculated from the Mediterranean salinity anomaly in the North Atlantic Ocean. *Journal of Physical Oceanography*, **5**, 173-182.

NOF, D. (1981) On the β-induced movement of isolated baroclinic eddies. *Journal of Physical Oceanography*, **11**, 1662-1672.

O'GARA, R.M., H.T. ROSSBY and D.L. SPAIN (1982) SOFAR float pilot studies in the western North Atlantic 1975-1981. *University of Rhode Island Technical Report*, **82-3**, 160pp.

OWENS, W.B. (1984) A synoptic and statistical description of the Gulf Stream and subtropical gyre using SOFAR floats. *Journal of Physical Oceanography*, **14**, 104-113.

OWENS, W.B. (1991) A statistical description of the mean circulation and eddy variability in the northwestern Atlantic using SOFAR floats. *Progress in Oceanography*, **28**, 257-303.

OWENS, W.B. and M.E. ZEMANOVIC (1990) An exploration of the North Atlantic Current and its recirculation in the Newfoundland Basin using SOFAR floats. *Woods Hole Oceanographic Institution Technical Report*, **WHOI-90-32**, 144pp.

PRATT, L.J., J. EARLES, P. CORNILLON and J.F. CAYULA (1991) The nonlinear behaviour of varicose disturbances in a simple model of the Gulf Stream. *Deep-Sea Research*, **38**, Supplement 1, S591-622.

PRICE, J.F. and H.T. ROSSBY (1982) Observations of a barotropic planetary wave in the western North Atlantic. *Journal of Marine Research*, **40** (Supplement), 543-558.

PRICE, J.F., T.K. McKEE, W.B. OWENS and J.R. VALDES (1987) Site L SOFAR float experiment, 1982-1985. *Woods Hole Oceanographic Institution Technical Report*, **WHOI-87-52**, 289pp.

PRICE, J.F., T.K. McKEE, J.R. VALDES, P.L. RICHARDSON and L. ARMI (1986) SOFAR float Mediterranean Outflow Experiment: Data from the first year, 1984-1985. *Woods Hole Oceanographic Institution Technical Report*, **WHOI-86-31**, 199pp.

RICHARDSON, P.L. (1980) Anticyclonic eddies generated near the Corner Rise seamounts. *Journal of Marine Research*, **38**, 673-686.

RICHARDSON, P.L. (1983) Gulf Stream rings. Chapter 2. In: *Eddies in Marine Science*, A.R. ROBINSON, editor, Springer-Verlag, Berlin, 19-45.

RICHARDSON, P.L. (1985) Average velocity and transport of the Gulf Stream near 55°W. *Journal of Marine Research*, **43**, 83-111.

RICHARDSON, P.L., R.E. CHENEY and L.V. WORTHINGTON (1978) A census of Gulf Stream rings, Spring 1975. *Journal of Geophysical Research*, **83**(C12), 6136-6144.

RICHARDSON, P.L., M.S. McCARTNEY and C. MAILLARD (1991) A search for Meddies in historical data. *Dynamics of Atmospheres and Oceans*, **15**, 241-265.

RICHARDSON, P.L., D. WALSH, L. ARMI, M. SCHRÖDER and J.F. PRICE (1989) Tracking three Meddies with SOFAR floats. *Journal of Physical Oceanography*, **19**, 371-383.

RICHARDSON, P.L., J.F. PRICE, W.B. OWENS, W.J. SCHMITZ, Jr., H.T. ROSSBY, A.M. BRADLEY, J.R. VALDES and D.C. WEBB (1981) North Atlantic subtropical gyre: SOFAR floats tracked by moored listening stations. *Sciencez*, **213**, 435-437.

RISER, S.C. and H.T. ROSSBY (1983) Quasi-Lagrangian structure and variability of the subtropical western North Atlantic circulation. *Journal of Marine Research*, **41**, 127-162.

RISER, S.C., H.J. FREELAND and H.T. ROSSBY (1978) Mesoscale motions near the deep western boundary of the North Atlantic. *Deep-Sea Research*, **25**, 1179-1191.

RISER, S.C., W.B. OWENS, H.T. ROSSBY and C.C. EBBESMEYER (1986) The structure, dynamics, and origin of a small scale lens of water in the western North Atlantic thermocline. *Journal of Physical Oceanography*, **15**, 572-590.

ROBINSON, A.R., M.A. SPALL and N. PINARDI (1988) Gulf Stream simulations and dynamics of ring and meander processes. *Journal of Physical Oceanography*, **18**, 1811-1853.

ROSSBY, H.T., J. PRICE and D. WEBB (1986) The spatial and temporal evolution of a cluster of SOFAR floats in the POLYMODE Local Dynamics Experiment (LDE). *Journal of Physical Oceanography*, **16**, 428-442.

ROSSBY, H.T., S.C. RISER and A.J. MARIANO (1983) The western North Atlantic - A Lagrangian viewpoint. Chapter 4. In: *Eddies in Marine Science*, A.R. ROBINSON, editor, Springer-Verlag, Berlin, 66-91.

ROSSBY, H.T., A.D. VOORHIS and D. WEBB (1975) A quasi-Lagrangian study of mid-ocean variability using long-range SOFAR floats. *Journal of Marine Research*, **33**, 355-382.

SCHMITZ, W.J. Jr., (1985) SOFAR float trajectories associated with the Newfoundland Basin, *Journal of Marine Research*, **43**, 761-778.

SCHMITZ, W.J. Jr., J.F. PRICE and P.L. RICHARDSON (1988) Recent moored current meter and SOFAR float observations in the eastern Atlantic near 32°N. *Journal of Marine Research*, **46**, 301-349.

SCHMITZ, W.J. Jr., J.F. PRICE, P.L. RICHARDSON, W.B. OWENS, D.C. WEBB, R.E. CHENEY and H.T. ROSSBY (1981) A preliminary exploration of the Gulf Stream system with SOFAR floats. *Journal of Physical Oceanography*, **11**, 1194-1204.

SEAVER, G. (1987) Geographic and temporal eddy variability in the western North Atlantic as sensed by satellite: an eddy generation mechanism. *Journal of Physical Oceanography*, **17**, 1602-1618.

SHAW, P-T. and H.T. ROSSBY (1984) Towards a Lagrangian description of the Gulf Stream. *Journal of Physical Oceanography*, **14**, 528-540.

SPAIN, D.L., R.M. O'GARA and H.T. ROSSBY (1980) SOFAR float data report of the POLYMODE Local Dynamics Experiment. *University of Rhode Island Technical Report*, **80-1**, 200pp.

SPALL, M.A. (1992) Rossby wave radiation in the Cape Verde Frontal Zone. *Journal of Physical Oceanography*, **22**(7), 796-807.

SPALL, M.A. and A.R. ROBINSON (1990) Regional primitive equation studies of the Gulf Stream meander and ring formation region. *Journal of Physical Oceanography*, **20**, 985-1016.

SWALLOW, M. (1961) Deep currents in the open ocean. *Oceanus*, **7**, 2-8.

WOODING, C.M., W.B. OWENS, M.E. ZEMANOVIC and J.R. VALDES (1989) Gulf Stream Recirculation Experiment - Part II. *Woods Hole Oceanographic Institution Technical Report*, **WHOI-89-37**, 316pp.

WORTHINGTON, L.V. (1959) The 18° water in the Sargasso Sea. *Deep-Sea Research*, **5**, 297-305.

WORTHINGTON, L.V. (1976) On the North Atlantic circulation. *The Johns Hopkins Oceanographic Studies*, **6**, 110pp.

WORTHINGTON, L.V. (1977) Intensification of the Gulf Stream after the winter of 1976-77. *Nature*, **270**, 415-417.

ZEMANOVIC, M.E., P.L. RICHARDSON and J.F. PRICE (1990) SOFAR float Mediterranean Outflow Experiment: Summary and data from 1986-1988. *Woods Hole Oceanographic Institution Technical Report*, **WHOI-90-01**, 239+ivpp.

ZEMANOVIC, M.E., P.L. RICHARDSON, J.R. VALDES, J.F. PRICE and L. ARMI (1988) SOFAR float Mediterranean outflow experiment, data from the second year, 1985-1986. *Woods Hole Oceanographic Institution Technical Report*, **WHOI-88-43**, 230pp.

14. APPENDIX
LIST OF INDIVIDUAL LOOPERS

Each Looper identification number (SL124B-1, for example) contains two letters designating the experiment (SL), the float number in that experiment (124B), with different segments of a trajectory designated by letters (B), and the looper number of that float (1). Loopers were stratified first by region, then by rotation direction, and then by depth, and were given a consecutive number for easy identification in the text. The date, latitude, and longitude are for the beginning of each looper. Other values are summaries or averages over each looper series. An asterisk beside a temperature indicates the value was estimated from incomplete data. An asterisk beside a pressure indicates the value was either estimated from gappy data or was the target pressure at launch. The range of looper diameters in the parentheses was estimated visually from trajectories. V is the magnitude of the mean translation vector and θ the direction in degrees true, V_θ is the swirl velocity, and R_0 is the Rossby number, estimated from $2V_\theta/fD$. The text describes how the various quantities were calculated.

Looper Number	Float ID	Date	Duration (days)	Lat	Long	Temp (°C)	Pressure (db)	Number of loops	Period (days)	Swirl Velocity (cm/sec)	Diameter (km)	EKE (cm^2/sec^2)	u (cm/sec)	v (cm/sec)	V (cm/sec)	θ	V/V_θ	R_0
Western North Atlantic (North of 30N, West of 60W)																		
1	SL124B-1	850223	188	36.40	-52.77	15.00*	500*	17.8	10.5	41.6	120 (50-270)	863	-4.33	-1.41	4.55	252	0.11	0.08
2	SL124B-2	830918	133	30.76	-63.31	18.22	512	27.0	4.9	24.2	33 (20-100)	293	-1.05	0.95	1.42	312	0.06	0.20
3	RI7-1	741002	80	32.55	-69.37	-	530*	2.4	32.9	8.3	75 (30-80)	34	-4.55	1.06	4.67	283	0.56	0.03
4	SL138-1	840427	83	40.01	-55.85	6.80	630	2.3	35.7	15.9	156 (80-190)	127	-4.12	2.04	4.60	296	0.29	0.02
5	SL125A-1	830105	64	39.00	-65.72	5.97	657	4.2	14.8	25.8	105 (20-120)	333	10.93	2.68	11.25	76	0.44	0.06
6	SL126-1	821210	70	36.83	-66.66	6.13	662	7.9	8.6	27.2	64 (20-90)	369	-1.99	-2.28	3.03	221	0.11	0.10
7	SL133B-1	830904	97	36.97	-66.13	5.40	673	4.2	22.6	24.0	149 (30-230)	287	7.90	0.53	7.92	86	0.33	0.04
8	LD64-1	780818	27	33.99	-73.10	13.17	674	2.6	10.0	43.8	120 (100-160)	961	-3.23	-0.48	3.27	262	0.07	0.09
9	PL26B-1	780707	48	33.28	-72.89	15.00	679	2.4	19.6	29.3	158 (90-170)	430	-1.04	1.61	1.92	327	0.07	0.04
10	GU116A-1	810808	138	37.10	-54.90	9.25	685	4.2	32.2	19.3	170 (30-230)	186	-1.05	-2.86	3.05	200	0.16	0.02
11	SL142-1	840409	107	30.74	-68.56	13.41	690	4.0	26.5	5.9	43 (10-50)	17	-3.36	-1.20	3.57	250	0.61	0.04
12	LD55-1	790407	92	32.58	-71.04	14.24	693	4.9	18.2	34.1	170 (80-190)	583	2.25	3.26	3.96	35	0.12	0.05
13	SL139-1	840320	47	32.52	-74.46	12.51	693	2.6	17.7	14.6	71 (50-80)	107	1.52	4.10	4.37	20	0.30	0.06
14	LD84-1	780807	87	31.32	-70.32	12.55	698	4.6	18.7	14.9	77 (45-90)	111	-6.28	3.26	7.08	297	0.48	0.05
15	LD56-1	780511	68	31.47	-69.53	13.59	705	2.0	33.5	10.7	99 (70-100)	58	-7.95	0.05	7.95	270	0.74	0.03
16	SL132B-1	830919	56	36.49	-67.61	10.37	705	4.5	12.2	48.2	161 (140-190)	1163	-9.64	-5.96	11.33	238	0.24	0.07
17	SL132BC-1	840209	133	32.56	-70.65	11.62	707	5.7	23.2	18.3	116 (70-160)	167	-2.92	0.02	2.92	270	0.16	0.04
18	SL132C-1	850501	37	35.94	-64.98	11.46	707	4.0	9.2	47.3	119 (100-140)	1119	-3.30	-0.01	3.30	270	0.07	0.10
19	GU106-1	800531	361	40.02	-50.71	8.56	711	26.0	13.8	20.7	79 (20-200)	215	-1.95	-1.67	2.57	229	0.12	0.06
20	GU113-1	811005	63	38.84	-56.85	-	721	5.5	11.3	35.8	111 (30-180)	642	-1.93	-0.55	2.01	254	0.06	0.07
21	GU121-1	810920	59	34.20	-70.95	11.16	761	3.4	16.8	9.6	44 (20-70)	46	-3.34	-3.13	4.57	227	0.48	0.06
22	SL140-1	831015	48	38.11	-63.97	11.40	788	2.9	15.5	36.1	154 (130-180)	653	-7.04	-4.23	8.21	239	0.23	0.05
23	SL130B-1	830604	42	35.70	-68.13	13.21	888	3.0	13.7	37.8	142 (35-190)	713	-1.07	5.64	5.74	349	0.15	0.06
24	RI9B-1	750626	70	35.70	-68.81	-	990*	2.2	31.1	12.5	107 (75-175)	79	-2.33	-1.27	2.65	241	0.21	0.03
25	RI2-1	741005	55	32.70	-69.05	-	1050*	2.8	19.3	8.9	47 (20-70)	40	-5.36	1.41	5.54	285	0.62	0.05
26	LD38-1	790816	40	37.74	-64.53	4.00	1291	3.8	10.4	21.9	62 (20-150)	239	11.90	-0.09	11.90	90	0.54	0.08
27	LD38-2	781218	98	34.14	-73.17	4.97	1299	1.8	55.4	5.8	87 (80-100)	17	-0.37	0.16	0.40	293	0.07	0.02
28	LD41-1	781103	76	30.37	-70.28	4.84	1344	1.8	42.9	5.9	69 (50-90)	17	-1.31	1.35	1.88	316	0.32	0.02
29	MO39-1	741215	152	30.16	-73.13	-	1500*	32.5	4.6	17.8	23 (15-60)	159	-2.21	-0.23	2.22	264	0.12	0.22
30	GU169C-1	840603	74	37.07	-71.86	-	2000*	3.5	20.9	15.8	91 (30-130)	125	3.58	1.15	3.76	72	0.24	0.04
31	GU169C-2	841118	45	39.32	-58.48	-	2000*	1.9	23.2	16.6	105 (70-120)	137	2.75	1.23	3.01	66	0.18	0.04
32	GU170A-1	810715	114	34.63	-65.55	3.68	2130	3.5	32.3	8.1	72 (30-85)	33	-1.38	0.13	1.38	275	0.17	0.02
33	GU165D-1	840722	137	36.22	-56.52	3.70	2189	4.0	33.8	9.0	83 (35-140)	41	4.52	0.66	4.57	82	0.51	0.02
34	GU165D-2	840130	55	38.10	-55.99	3.50	2200*	1.7	31.8	13.4	117 (40-140)	90	-4.01	0.20	4.01	273	0.30	0.02
35	SL124B-3	840409	261	31.46	-65.73	15.00*	500*	23.5	11.1	-35.1	107 (75-120)	616	-2.25	2.77	3.57	321	0.10	0.08
36	LD54-2	790501	24	35.04	-65.84	15.70	679	3.5	6.6	-23.6	43 (30-50)	278	9.85	3.40	10.42	71	0.44	0.13
37	SL124AB-1	830310	74	36.39	-66.95	18.00*	679	6.6	10.9	-38.0	107 (40-170)	646	2.82	-1.81	3.35	123	0.09	0.08
38	SL143-1	830916	42	40.05	-58.40	10.68	683	3.0	13.7	-34.4	129 (130-140)	591	-1.61	1.71	2.35	317	0.07	0.06
39	LD54-3	780913	156	34.00	-73.79	14.86	695	5.5	28.2	-14.1	109 (10-130)	100	1.02	1.26	1.62	39	0.11	0.03
40	LD32-1	780520	19	31.54	-68.98	-	700*	2.5	7.6	-10.8	22 (15-25)	58	-3.27	0.12	3.27	272	0.30	0.12
41	LD61-1	780620	29	32.50	-73.21	15.75	706	2.8	10.2	-37.3	104 (90-115)	696	-6.33	-1.68	6.55	255	0.18	0.09
42	LD55-2	781009	59	32.67	-74.26	14.72	706	1.7	34.1	-19.6	183 (135-200)	192	0.84	-0.38	0.92	114	0.05	0.02
43	LD54-4	780610	54	32.63	-71.17	14.62	711	2.0	26.5	-29.5	214 (140-240)	436	-4.45	0.37	4.47	275	0.15	0.04
44	SL142-2	831022	159	33.39	-70.65	13.93	712	16.5	9.6	-18.4	48 (40-50)	169	2.12	-1.56	2.63	126	0.14	0.10
45	SL132B-2	831114	31	33.60	-72.86	14.20	743	2.8	10.9	-36.6	109 (40-160)	670	-3.41	2.81	4.42	309	0.12	0.08
46	GU102-1	800430	152	32.02	-55.08	13.07	744	6.8	22.4	-25.2	155 (90-160)	318	-4.02	0.02	4.02	270	0.16	0.04
47	LD52-1	780513	75	30.97	-69.50	12.18	748	21.0	3.5	-20.0	19 (10-20)	199	-4.82	-5.05	6.98	224	0.35	0.28
48	SL132B-3	830621	49	33.69	-65.78	13.23	752	1.8	26.7	-9.6	70 (40-100)	46	1.22	-3.67	3.87	162	0.40	0.04
49	SL127A-1	821126	46	35.00	-70.61	15.86	799	3.8	11.8	-27.9	90 (25-120)	389	7.85	1.64	8.02	78	0.29	0.08
50	SL131A-1	830214	78	33.75	-70.86	13.72	805	3.4	22.6	-19.3	120 (40-250)	187	0.36	2.34	2.37	9	0.12	0.04
51	LD51-1	780515	41	30.81	-69.43	5.01	1256	1.7	23.5	-13.5	87 (35-90)	91	-4.63	-4.31	6.47	228	0.28	0.04
52	LD50-1	780513	44	30.88	-69.40	4.77	1299	3.8	11.3	-17.4	54 (10-60)	151	-4.19	-4.10	5.86	226	0.34	0.08
53	LD58-1	780514	104	30.98	-69.24	-	1500*	6.5	15.8	-13.4	58 (20-60)	90	-2.13	-0.36	2.16	260	0.16	0.06
54	GU164-1	820105	61	40.04	-51.57	-	1803	6.2	9.7	-13.5	36 (30-50)	91	-2.22	2.00	2.99	312	0.22	0.08
55	GU166-1	810809	80	36.16	-54.96	-	2000*	3.0	26.0	-7.7	55 (50-100)	30	2.96	2.00	3.57	56	0.46	0.04
56	GU167B-1	830714	71	33.52	-61.28	-	2004	4.5	15.6	-9.0	39 (20-40)	41	-4.01	6.47	7.62	328	0.85	0.06
57	GU165D-3	850406	49	35.00	-56.43	3.55	2137	1.8	27.4	-10.6	80 (45-100)	56	-0.45	0.75	0.87	329	0.08	0.03

Looper Number	Float ID	Date	Duration (days)	Lat	Long	Temp (°C)	Pressure (db)	Number of loops	Period (days)	Swirl Velocity (cm/sec)	Diameter (km)	EKE (cm^2/sec^2)	u (cm/sec)	v (cm/sec)	V (cm/sec)	θ	V/V_θ	R_0
Western North Atlantic (South of 30N, West of 60W)																		
58	PL14-1	760603	24	23.44	-72.94	11.02	689	2.0	11.5	11.7	37 (25-45)	69	-4.88	3.65	6.09	307	0.52	0.11
59	PL25-1	790118	51	26.20	-71.52	11.70	689	2.0	25.0	12.7	87 (70-90)	80	-6.92	-2.80	7.46	248	0.59	0.04
60	LD59A-1	780909	85	25.66	-75.77	12.26	691	3.4	24.7	20.4	138 (80-140)	207	2.26	3.10	3.84	36	0.19	0.04
61	LD59A-2	781212	117	27.37	-73.01	12.55	695	4.5	25.3	13.5	93 (30-120)	91	-2.44	3.07	3.92	322	0.29	0.04
62	PL21F-1	790228	98	27.27	-74.42	11.45	697	6.3	15.6	19.7	84 (20-175)	195	-1.83	1.61	2.44	311	0.12	0.07
63	PL22-1	770215	62	26.84	-71.71	12.28	699	3.2	19.7	5.9	32 (15-35)	17	-2.50	-1.60	2.97	237	0.50	0.06
64	PL21E-1	781109	53	24.57	-73.70	12.00	699	3.5	14.9	14.6	60 (30-70)	109	-4.30	5.29	6.82	321	0.46	0.06
65	SL123B-1	840822	41	29.10	-76.70	6.87	700*	1.9	21.1	15.1	87 (60-100)	114	1.98	-2.65	3.31	143	0.22	0.05
66	MO46A-1	741207	135	29.89	-72.48	-	1500*	10.9	12.3	14.1	47 (20-75)	99	-2.48	0.69	2.57	286	0.18	0.06
67	MO37BC-1	760217	79	27.35	-74.36	-	1500*	7.9	9.8	16.3	44 (30-60)	133	-2.57	-2.01	3.26	232	0.20	0.11
68	PL29-1	780731	161	24.71	-67.53	3.60	1999	5.5	29.1	9.0	72 (65-85)	41	-0.71	0.86	1.12	320	0.12	0.04
69	GU170E-1	840830	114	22.38	-71.51	-	2000*	3.0	37.7	7.1	73 (30-75)	25	3.48	-2.53	4.30	126	0.61	0.04
70	PL14-2	761215	166	24.21	-70.95	10.74	692	13.6	12.1	-18.0	60 (35-130)	162	-1.24	-1.05	1.62	230	0.09	0.10
71	PL14-3	761004	46	24.71	-68.94	13.16	700*	2.7	16.7	-23.2	106 (80-110)	269	-6.75	-2.63	7.24	249	0.31	0.07
72	PL9F-1	800418	109	20.17	-66.54	-	700*	2.0	55.0	-11.9	180 (150-180)	71	-1.73	0.05	1.73	272	0.15	0.02
73	GU107-1	800502	77	27.08	-55.13	11.52	718	2.6	30.0	-6.2	51 (20-70)	19	-4.51	-1.54	4.76	251	0.77	0.04
74	PL11B-1	770625	99	23.26	-67.20	-	827	3.8	26.1	-8.4	60 (40-70)	35	-1.09	0.51	1.20	295	0.14	0.05
75	PL12A-1	761004	65	24.36	-69.04	10.40	850*	6.5	9.8	-7.9	21 (15-25)	31	-6.48	-2.49	6.94	249	0.88	0.12
76	PL12B-1	770308	50	24.80	-74.17	6.59	850*	2.2	22.7	-11.7	73 (60-80)	69	2.65	-3.59	4.46	144	0.38	0.06
77	PL27-1	780924	34	27.97	-76.48	3.61	1998	4.9	6.6	-21.6	39 (20-40)	234	6.23	-13.30	14.70	155	0.68	0.16
Newfoundland Basin																		
78	NB99V-1	871210	36	45.46	-44.29	4.21	637	2.4	14.6	13.4	54 (10-60)	89	-2.62	-4.55	5.25	210	0.39	0.05
79	GU116A-2	820709	126	32.90	-39.23	9.53	654	2.2	55.6	10.2	156 (100-160)	52	-1.13	2.39	2.64	335	0.26	0.02
80	GU116A-3	830115	108	38.55	-43.27	8.46	666	3.5	30.6	16.2	136 (30-160)	131	-0.57	-1.92	2.00	196	0.12	0.02
81	NB99-2	870618	56	44.47	-45.06	3.99	668	2.2	24.4	8.4	56 (25-60)	35	-2.53	-2.38	3.47	227	0.41	0.03
82	GU110-1	801130	74	42.10	-38.52	7.42	671	2.0	36.5	10.4	104 (100-110)	54	-1.75	-0.12	1.76	266	0.17	0.02
83	NB99-3	880127	176	41.65	-41.72	6.67	678	13.5	13.0	18.8	67 (10-180)	177	0.81	-1.38	1.60	150	0.09	0.06
84	SL143-2	840206	140	39.60	-44.91	10.11	688	5.1	27.3	25.1	189 (100-200)	317	2.41	0.09	2.41	89	0.10	0.03
85	NB99-4	861010	51	51.22	-43.31	3.62	698	4.7	10.6	17.9	52 (15-60)	160	0.28	-0.11	0.30	111	0.02	0.06
86	NB99-5	860629	96	49.61	-42.09	3.83	707	7.5	12.7	16.3	57 (40-100)	133	-2.51	0.49	2.56	281	0.16	0.05
87	NB93A-1	861129	277	39.24	-40.43	7.30	721	14.7	18.7	16.5	84 (20-130)	136	-0.82	-0.74	1.10	228	0.07	0.04
88	NB91-1	860602	102	40.91	-40.11	7.28	732	7.2	13.8	20.1	76 (40-80)	202	-2.30	-0.63	2.38	195	0.12	0.06
89	NB94-1	861012	121	46.22	-41.81	5.07	745	4.9	24.5	18.4	124 (20-220)	170	3.57	-1.22	3.77	109	0.20	0.03
90	GU120A-1	811005	149	41.48	-46.31	10.00*	800*	8.9	16.4	21.9	99 (30-180)	240	3.55	4.59	5.80	38	0.26	0.04
91	GU163B-1	830605	67	39.54	-49.46	3.68	2097	3.2	20.6	16.4	93 (60-100)	134	0.35	1.14	1.19	17	0.07	0.04
92	GU156-1	801012	139	39.12	-49.05	3.70	2191	6.6	20.9	16.1	92 (30-140)	129	-0.58	0.90	1.07	328	0.07	0.04
93	NB94-2	870501	180	40.14	-33.46	11.15	671	6.9	25.6	-18.0	126 (60-230)	162	-3.08	-1.79	3.56	240	0.20	0.03
94	GU109A-1	801021	62	46.32	-39.65	10.30*	700*	12.9	4.7	-31.8	41 (15-200)	504	-1.02	3.31	3.46	343	0.11	0.14
95	NB99-6	880722	86	40.53	-40.74	11.29	705	3.5	24.3	-20.9	139 (20-190)	217	-2.91	-2.31	3.72	232	0.18	0.03
96	NB99-7	870102	59	50.14	-42.68	5.13	712	7.1	8.3	-39.9	91 (50-150)	797	0.03	2.31	2.31	1	0.06	0.08
97	NB93A-2	860705	43	42.55	-38.95	8.19	833	3.0	14.0	-22.5	86 (45-110)	253	-3.01	-0.14	3.01	183	0.14	0.06
98	NB96-1	861115	131	44.79	-39.50	4.60	1150	4.0	32.5	-8.7	78 (20-150)	38	-2.05	0.84	2.22	292	0.26	0.02
Eastern Basin																		
99	EB014A-1	870223	261	32.83	-27.54	-	220*	9.9	26.0	13.0	93 (20-150)	85	-3.44	-0.05	3.44	269	0.26	0.04
100	EB127A-1	850603	63	32.68	-28.32	8.30	1090	4.5	13.8	6.8	26 (15-30)	23	-0.34	2.16	2.19	351	0.32	0.06
101	EB144-1	851013	46	20.54	-19.08	-	1200*	2.3	19.6	8.0	43 (30-45)	32	0.56	-2.15	2.22	165	0.28	0.08
102	EB148-1	860807	41	31.06	-28.75	8.46	1193	3.7	10.8	7.4	22 (10-40)	28	-0.18	-1.85	1.86	186	0.25	0.09
103	EB128-1	841016	821	32.03	-22.13	10.32	1118	114.0	7.2	-12.8	25 (5-50)	83	0.02	-1.48	1.48	179	0.12	0.13
104	EB140-1	841018	117	32.01	-21.95	10.86	1200*	20.0	5.9	-7.6	12 (5-30)	29	-0.14	-2.17	2.17	184	0.29	0.16
105	EB141-1	841018	234	31.93	-22.15	10.95	1018	41.0	5.7	-7.6	12 (5-40)	29	-0.45	-1.72	1.78	195	0.23	0.16
106	EB143-1	841018	269	31.90	-22.20	11.27	1146	47.0	5.7	-9.8	15 (5-20)	48	-0.43	-1.85	1.90	187	0.19	0.16
107	EB145-1	850919	549	24.28	-23.39	8.11	1143	54.0	10.2	-9.8	27 (5-80)	48	-0.44	-0.96	1.06	204	0.11	0.12
108	EB148-2	851114	267	33.99	-24.25	11.78	1143	57.0	4.7	-17.4	22 (10-30)	151	-1.79	-1.40	2.27	232	0.13	0.19
109	EB149-1	851114	262	33.92	-24.17	12.42	1032	62.0	4.2	-14.2	16 (10-50)	101	-1.97	-1.36	2.40	235	0.17	0.22
110	EB150-1	851101	170	26.98	-23.52	8.15	1200*	8.1	20.9	-6.0	34 (30-40)	18	-0.28	-1.33	1.36	192	0.23	0.06
111	EB131-1	841022	125	32.42	-24.27	8.18	1145	4.4	28.2	-3.7	29 (20-30)	7	-1.70	-0.49	1.77	254	0.48	0.04
112	EB133-1	850813	110	32.33	-29.67	8.57	1102	3.0	36.3	-7.5	75 (45-85)	28	-3.91	-1.23	4.09	253	0.55	0.02
113	EB137-1	850709	71	31.74	-29.16	8.84	1097	2.0	35.0	-8.3	80 (80-80)	35	-3.38	-1.09	3.55	252	0.43	0.02
114	EB137-2	860601	318	31.67	-33.61	8.65	1090	12.5	25.2	-5.6	39 (10-100)	16	-2.19	-0.73	2.31	252	0.41	0.04
115	EB134-1	850203	49	35.07	-20.44	6.97	1200*	3.9	12.3	-2.0	7 (5-7)	2	-0.14	1.79	1.79	356	0.89	0.07
116	EB144-2	850921	21	20.65	-18.51	-	1200*	1.9	10.5	-13.2	38 (20-40)	87	-2.14	-0.12	2.14	273	0.16	0.14
117	EB148-3	861007	80	30.66	-28.58	8.27	1178	5.9	13.2	-5.3	19 (10-30)	14	-1.04	1.03	1.46	315	0.28	0.08
118	EB149-2	870106	59	31.96	-29.02	8.48	1017	2.5	23.2	-6.8	43 (20-50)	23	-0.14	1.57	1.58	355	0.23	0.04